Final Report for the Project FST-D-ISR-10

An Ultrashort-X-Ray Emission from Gas Clusters Irradiated by Ultrashort Laser Pulses

FKZ: 13N7961

I..Short project presentation

I.1.1. Overall objectives

The microelectronics industry starts to face resolution limits of the present technology and it has to be decided in the nearest future (likely in the perspective of 5 to 6 years) which of two source technologies, i.e. either discharge or laser plasma, is the best one and should be implemented in the new short-wavelength lithography. On the other hand life and material sciences need also a deep look into the nano-and femtoworld. A short-wavelength and in some cases short-pulse source is of paramount importance for each of these applications as this dominantly decides about the spatial and temporal resolutions. It is expected that both, coherent and incoherent soft X-ray sources could help to solve many of the problems faced.

Laser plasmas are very attractive as soft X-ray sources for projection lithography, microscopy, interferometry and many others applications due to their compactness, flexibility and simplicity. Much work on such incoherent sources has been done during the last decade, mostly on classic gas and solid state targets interacting with long, nanosecond laser pulses. If reliable and reproducible, such a source could be interesting for the industrial applications. One decade ago clusters received, as one of the possible targets, attention of several studies and the number of publications exploded in the last few years as they combine in an unique way features of both solids and gases. As a consequence, they promise high conversion efficiency of the solids and strongly limited contamination of the x-ray optics due to nearly debris-free work, typical for gases. In some extreme cases it could be spoken about a hot nanoplasma.
Our main goal is to obtain well characterised, efficient source, working with increased (min. 10 Hz) repetition rate in the spectral range between 10 and 15 nm, where relatively efficient X-ray optics exists. Plasma in two different excitations schemes is to be investigated:

a. Optical-field-induced ionization (OFI) appeard as an experimental fact with the advent of high intensity low energy fs-lasers. This method of the plasma creation started to be applied to the x-ray sources dedicated to the practical applications only recently. Using polarisation, wavelength and pulse length dependent state of the plasma created we hope to influence and exactly control the spectra emitted and the same to match the parameters of emitted radiation to the x-ray optics and potential application requirements. Both, clusters and dense gases are foreseen as targets.
b. Collisional ionisation of the clusters initiated by pico- and nanosecond laser irradiation.

One of the most important aspects of the sources applicable in practice is the target preparation to ensure high directionality, required spectral content, good beam quality of the output radiation and reasonable interaction volume. For this reason we are going to check possibility to confine the cluster medium in a capillary. Such a confinment should also improve the output beam divergence and directionality.

It was shown recently by both hydrodynamic simulations and experimental spectral analysis, that a cold homogeneous optically thin plasma core, close to solid density, can be created at early phase of the interaction, where hydro-dynamical changes had not been strongly developed yet. This core localized in both space and time is therefore an optically thin LTE source of radiation with well defined density and a relatively small temperature spread of no more than 150 eV. This plasma state was to be investigated in detail. We are also going to extend some previous results on a fine energy tuning within the 3d-shell of high-Z materials to the caplillary confined Xe cluster in order to localize X-ray emission and to obtain high brightness which is a dominant consideration in the design of efficient X-ray source.
As incoherent XUV-sources at higher repetition rate influence strongly the X-ray optics and the bandwith problems start to be crucial for the system performance we were going to check in a suplementary experiment also coupling efficiency to the x-ray optics, if a coherent, narrow-bandwith source as Ni-like Ag X-ray laser at 13.9 nm is used. This X-ray laser is at the moment a single-shot type device, but a combination of the X-ray laser and X-ray optics in the spectral range between 10 and 15 nm could effectively be checked already now.

I.1.2. Scientific and technical goals

A very rich world of cluster structures delivers a new fascinating phenomena in interaction with an intense laser radiation. There existed some controverses regarding the absorption mechanisms and fast expansion of the clusters (Coulomb explosion or hydrodynamic driven). There were still uncleared differences in behaviour between the big (a few hundreds tousends of atoms) and small (a few hundreds of atoms) clusters. At the same time an unique feature combining solid and gas states in one temptated to use clusters als a target material to increase efficiency of the energy transformation into repetitive short-wavelength bursts. The radiation emission being a function of the state of the plasma created in the interaction process could be controlled by the parameters of the pumping radiation. The pulse length, its peak intensity and polarisation state determine the resulting plasma temperature and the electron distribution function, which are deciding for the excitation and subsequent emission processes. Having changed polarisation state between the linear and circular one we are able to move, in the case of dense gases, from a bi-Maxwellian electron energy distribution (cold plasma) to a plasma combination of near-monoenergetic components (hot plasma). This dependence for the clusters is weeker, less explored and understood. A well characterised plasma state being the interaction effect and the resulting emission of a short-wavelength radiation were main goals of this part of the project. The ultimate target, interaction scheme and and the output characteristics of the source will be determined in the coarse of the project as a result of the comparative analysis. A major experimental effort has to be put in the technological development. The clustering level of Xe-clusters has to be monitored by the Rayleigh scattering. Cooling by only the gas expansion could be insufficient in some cases and cryogenic gas jets has to be involved. Deeply cooled gas jets require very reliable and sofisticated high vacuum system. The focusing system has to ensure maximal interaction length at required laser pulse intensity. Thus the focusing system and its position relative to the cluster launch have to be analysed and optimised. Another possibility being subject to the experimental check is applying a capillary for the cluster confinement. This probably the most challenging part of the project. If succeeded, directionality of the soft x-ray output should be improved in a remarkable way. The pump laser system is source of another challenge. Stability ist extremely important for the system working as a pumping source. The repetiton rate has to increase to obtain significant value of the average power.
As any incoherent source emits within a broad bandwith which is significantly broader than the bandwith of the x-ray optics elements, there appears a danger that this optics could be overloaded (overheated). It is an interest to develop coherent sources with a narrow bandwith

matching that of the optics available. For this reason we are going to check possibility to use an Ni-like Ag soft X-ray laser and estimate its coupling efficiency to the x-ray optics. If succeed much effort could be focused on the stability improvement which is in turn strongly dependent on the stability of the optical laser driver. The latter is at the moment a single shot device and increase of the repetition rate would be required. This would be a new impact on the development of both the x-ray lasers and classic drivers at visibleand NIR wavelentghs. Due to the extremely hard constraints on the industrially applicable sources the investigation should be focused on the broad spectrum of targets and interaction methods to give a rich information about the potential way to the commercial source in the future.

I.1.3. Relevance to the goals of the funding programm

The most general goal of the funding programme is support of the precompetitive research in the field of femtosecond technology (FST). In the project are included both generation and characterisation of ultrashort radiation pulses at soft XUV spectral range which could be applied in the life and material sciences. Significant effort has been recently put into development of radiation sources with extreme short wavelength and duration time. Such sources would be beneficial not only for the microlitography but also in x-ray microscopy, reflectometry and time-resolved X-ray applications in different branches of technology and science. Thus, the development of such radiation source belongs to work on the leading front of applied sciences and requires interdisciplinary cooperation and application highly sofisticated technologies.

I*.2. Pre-conditions of the conducted research*

Chances of success during the main phase of the project, i.e. creation and optimising of a soft X-ray source from Xe-clusters, were good but required much effort put into the technological development. The target, i.e. the Xe cluster is well known and object of extensive investigations giving much of the reference material. Our lab was well equipped regarding diagnostic and the irradiating sources and the staff was experienced in the spectroscopic investigations under high-intensity irradiation. The interaction chamber together with the cooled cluster launch were constructed in the preparation phase. The attempt to confine the clusters in a capillary was absolutely new, and considered as an alternative one. This was also the most difficult technological part of the project. However, the Hebrew University group is very experienced in the dense plasma investigations both experimentally and theoretically.
The second part of the project was planned as a preliminary experiment which could have, if succeeded, enormous impact on the soft X-ray sources development. Moreover, it would give new pulses in the CPA-laser system development. However, the risk to fail was higher as the X-ray laser output was less known. We expected from the Ag-XRL a few microjoules of the output energy and intensity $\sim 10^{10}$ W/cm^2. The durability and quality of the available x-ray optics were also unknown.

I.3. Operations planning

I.3.1 Work packages

WP1
Cluster beam production with well determined and controlled parameters. Cooled jets and their influence on cluster creation. Development of the cluster dimension diagnostic (Rayleigh scattering). Preparation of the spectral measurements on the clusters and the plasma of the post-expansion phase.

WP2
Comprehensive measurements on the plasma parameters and spectral emission of Xe-clusters created under different conditions. These conditions are determined by the cluster dimensions, laser wavelengrth, laser pulse length, intensity and polarisation. The spectral range of the emission includes both soft X-ray emission between 10 and 15 nm and the resonance lines below 4 nm. Temporally resolved spectra will be obtained with a X-ray streak camera.

WP3
Characteristics of a dense, temporally and spatially localized, optically thin LTE plasma with a cold core. The techniques applied in WP2 will be applied here to the plasma in a free space and Xe-clusters confined in a capillary. Some specific techniques from the investigations of an ionized high-Z material will be applied to obtain fine tuning of the transition energy within the 3d-shell.

WP4
We are going to use Ag soft X-ray laser working at 13.9 nm in Ni-like ions and determine optical characteristics of its output beam (dimensions, divergence, intensity distribution, coherence) and subsequently couple this beam to the X-ray optics. The energy of a few microjoules and peak intensity of 10^{10} W/cm^2 are expected. Thus, some quasi-coherent source would be available for some applications.

I.3.2. Project schedule

Work package	Completed
WP1	30.06.2001
WP2	28.02.2002
WP3	31.12.2003
WP4	31.12.2002

The deadlines include time necessary to process the data obtained in the experiment.

I.3.3. Milestones

- Xe cluster producing from a cryogenic source (1st half of 2001)
- spectral investigation of the irradiated clusters (2001), conversion efficiency for some important emission lines (2001)
- creation of the dense, cold, optically thin high-Z plasma (end 2002)
- checking of the cluster confinment and emission from high density plasma (2002)
- coupling efficiency between the Ag x-ray laser and x-ray optics (end 2002)
- determination of the brightnes of the optimum scheme (mid 2003)
- Additionally: amplification in a recombining plasma- lasing

I.4. Scientific and technical state-of -the-art

The soft X-ray sources for the application, have extensively been developed during the last decade. While requirements which any applicable source has to fulfil are relatively well defined the way towards such a source is still not found. The incoherent sources were and are

the main stream of the investigations as x-ray lasers are at the moment not sufficiently stable and even if suitable energetically then are operating in a single pulse regime. One of the major limitation for the soft x-ray sources is debris effect being danger due to the x-ray optics contamination. This effect eliminates, in fact, solid targets from the race even if they offer relatively high conversion efficiency. Clusters turned recently common attention as a potential very efficient source of the soft x-rays if irradiated with ultrashort laser pulses, i.e. also with increased repetiton rate. First experiments conducted mainly on Xe confirmed potential of this element as a possible target. However, these experiments concentrated mostly on the the particle emission or extreme short-wavelength radiation and hardly exploited the pumping with pulse lengths about and shorter than 100 fs for emission investigation in the soft XUV spectral range [1]. The number of publications on cluster interaction increases with enormous rate. However, the plasma created by very short laser pulses after the big clusters expansion is not sufficiently charactertised up to date. The pulses below 100 fs were used to irradiate only very small clusters [2]. The data regarding emission features of a very dense plasma is very sparse. Using the dense plasma with a cold core we are going to access a new class of the interaction applying table-top femtosecond pump lasers. The work within this project could help to make a few very important steps forward in understanding of radiative features of the dense plasmas.
The MBI group has a long-standing experience in laser development and laser plasma research and therefore necessary driver lasers and corresponding diagnostics could be used in the frame of the project. The israelic group has brought into the project its experience in plasma spectroscopy and especially its discharge capillary arrangements, which where also crucial for several important topics investigated.

Patent situation

The single shot-pumped X-ray laser has already been patented (pending) by the MBI group and the support of this grant has helped to characterise fully the patented source.Some of the X-ray sources proposed earlier by other groups, for example liquid targets in the form of droplets, have already been patented.

I.5. Cooperation

The comprehensive scientific program included in the proposal required broad cooperation to realize the plans. The group cooperated with several other external groups working on spectrometer development and calibration (for example Bessy II, Berlin, group of Prof. Wilhein Remagen, Dr. A. Egbert LZH Hannover a.o.) as well as with internal MBI groups working on cluster creation and pump laser drivers with high repetition rates and specific diagnostics.
Members of both project groups visited partner's laboratory and took part in common experiments.

II. Detailled report

II.1 Scientific results

WP 1
Cluster beam production with well determined and controlled parameters. Cooled jets and their influence on cluster creation. Development of the cluster dimension diagnostic (Rayleigh

scattering). Preparation of the spectral measurements on the clusters and the plasma of the post-expansion phase.

Cluster creation and characterization

For the cluster beam production and its characterization as well as for the x-ray emission measurements (see WP 2) an experimental-setup was developed, which is shown in Fig. 1. The experiments have been mainly carried out with 50 fs laser pulses at 800 nm center wavelength from a 10 Hz repetition rate multi–TW Ti:Sa laser [3] at Max–Born–Institute. We used a 4 TW (200 mJ) beam of 60 mm in diameter, which was delivered via evacuated tubes from the vacuum compressor chamber to the interaction chamber. The beam is focused with an f/2 off-axis parabolic mirror having a focal length of 155 mm. The focus size was determined by imaging the attenuated beam onto a normal video 8 bit CCD-camera. With a beam waist of w_0 = 5 mm and the estimated energy content in a spot of a $d = 2w_0$ diameter an interaction intensity of ~ 2×10^{18} W/cm^2 was inferred. This intensity level was verified under comparable conditions in single atom ionization experiments [4]. The Xe–cluster target was formed by expanding the gas from pressures up to 55 bar and temperature of T_0 = 300 K through a hypersonic conical nozzle with a cone angle $2\theta = 7^o$, throat diameter of 400 mm and an 8 mm long conical section. For the target optimization and system synchronization the cluster beam is pulsed by an electromagnetic valve for every 3 sec with a pulse duration of 5 ms, which keeps the background pressure before each gas pulse on a 10^{-6} mbar level. The laser focus is placed approximately 1 mm below the orifice of the nozzle and the laser beam axis crosses the cluster beam at right angle.

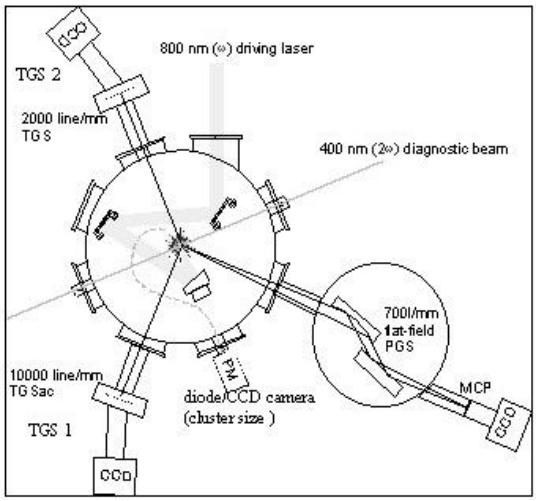

Figure 1: Experimental setup: Target and diagnostic setup for the Xe-cluster experiment. Focussing for the 800 nm Ti:Sa short pulse experiment (50fs) was done with an off-axis parabolic mirror (for the long ns-laser pulses at 1064 nm an aspherical lens was applied). The single shot plane grating spectrograph (PGS) was used in alignement procedures. The 400 nm diagnostic pulse was applied for an interferometry of the Xe-plasma

Soft x–ray spectra were measured with two transmission grating spectrometers and one flat field grazing incidence spectrometer allowing us the simultaneous registration of x–ray emission at different angles relative to the incident laser beam axis. One transmission grating spectrometer (TGS 2, on–axis) is looking at the target along the laser beam in axial. direction (grating 2000 l/mm, resolution $\lambda/\Delta\lambda$= 60 at 13 nm) covering the spectral region 5 – 20 nm. At

135° to the laser beam axis a second transmission grating spectrometer (TGS 2, off-axis) was installed (grating 10000 l/mm, resolution $\lambda/\Delta\lambda$ = 300 at 13 nm, comparable to those described in [5]), which was calibrated in absolute terms in the wavelength range between 10 nm and 15 nm at the synchrotron facility BESSY II (PTB – beamline). In both cases the spectra are registered with back-illuminated thinned 512×512-pixel CCD x-ray cameras (Photometrics, Scientific Instruments).
Optical light is blocked with 200 nm Zr filters. We integrated the spectra over 9 laser shots for quantitative analysis although it was also possible to monitor the x–ray emission on each shot. A third flat field grazing incidence EUV spectrograph with a varied spacing grating (average spacing 700 l/mm, resolution $\lambda/\Delta\lambda$= 300 at 13 nm) was used at the same angle as the TGS1 acting in single shot mode for qualitative comparison of the EUV-emission within target and laser beam alignment. Here the detection system is realized with a multichannel plate – phosphorous screen combination, which is red out with an optical sensitive CCD – camera.

Cluster size characterization
The clusters in the beam were formed by adiabatic expansion of a supersonic gas through a pulsed conical nozzle in to vacuum. Thermal energy is transformed into directed kinetic energy and the gas becomes overcritical and condensates. This behaviour can be characterized by the condensation scaling parameter G* of Hagena [6,7] allowing to compare different nozzle geometries:

$$\Gamma^* = k\frac{(d/\tan\alpha)^{0,85}p_0}{T_0^{2,29}} \tag{1}$$

with d- nozzle ∅ (mm), α-expansion half angle, p_0-backing pressure (mbar), start temperature T_0 (°K).

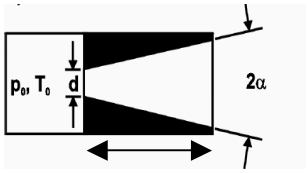

Figure 2: Hypersound nozzle, a = 3.5°, d = 400mm, l = 7mm

It follows from equation (1) that the cluster size increases with gas pressure p_0 and decreasing temperatur T_0. The empirical constant k in the Hagena formula increases with Z and it holds for different atoms: He (k=4), Ar (1700), Kr (2900) and Xe (5500). With other words, with the empirical constant k the cluster size depends on material: low Z-atoms create favourably small clusters and high Z-atoms large clusters. Employing Hagenas formula from [7] and the concept of equivalent nozzles a value of 2×10^6 atoms/cluster at 5 bar is derived.
The setup for the cluster creation (nozzle cross-section) is depicted Figure 2. The velocity v of the gas jet below the nozzle for monoatomic gases with atom mass m is given by [6]:

$$v = 2,98\cdot\delta^{2/3}\sqrt{\frac{2k_BT_0}{m}} \tag{2}$$

d- reduced distance to source and depends on the distance x to the nozzle (a- half opening angle of nozzle cone):

$$\delta = \frac{x}{0,74(d/\tan\alpha)} \tag{3}$$

The gas density at this point is

$$n = 0,15\cdot n_0\delta^{-2} \tag{4}$$

n_0- gas density in reservoir determined by temperature and backing pressure:

$$n_0 = 7,242 \cdot 10^{21} (p_0/bar)(K/T_0) \frac{\text{Atome}}{\text{cm}^3} \tag{5}$$

The characteristic parameters for the used nozzle geometry are given in table 1

Table 1. Characteristic parameters of the used nozzle for a temperature of 300°K. The density values n for the 3 different gas pressures are estimated at a distance of 2mm below the nozzle (i.e. x =9 mm).

α	d	v	p	n
3,5°	400 μm	878 m/s	5 bar	5,2·10^{18} Atome/cm^3
3,5°	400 μm	878 m/s	20 bar	2,1·10^{19} Atome/cm^3
3,5°	400 μm	878 m/s	35 bar	3,7·10^{19} Atome/cm^3

As already mentioned, the cluster size was determined by light scattering measurements (Rayleigh scattering). In principle are relative measurements [8] by this method rather simple, an absolute determination is however connected with some uncertainties [9]
If the radius r of the scattering particles is smaller than wavelength l of the scattered light, i.e. r / l << 0.05 [10] one can use the Rayleigh-theory for dielectric spheres. In this case is the cross section s for a single particle with volume V given by [10,11]:

$$\sigma = \frac{128\pi^5 r^6}{3\lambda^4} \left(\frac{n^2 - 1}{n^2 + 2} \right)^2 \sim \frac{V^2}{\lambda^4} \tag{6}$$

n- refraction index of the particles. The Rayleigh scattering has an $1/\lambda^4$ dependence (blue sky !). For an ensemble of N particles, which are independent each i.e they are scattering incoherently, one can obtain a cross section by multiplying the cross section for single particle s with particle number N.
In a first step it is possible to check qualitatively, whether clusters are created or not. The scattered signal I_s to be measured depends on the impinging radiation I_o, the cluster number N_{clust} and number of atoms per cluster $N_{at/clust}$ as follows:

$$I_S \sim I_0 \cdot N_{clust} \cdot V_{clust}^2 \sim I_0 \cdot N_{clust} \cdot N_{at/clust}^2 \tag{7}$$

From other experiments it is known , that $N_{at/clust}$ scales quadratically with backing pressure p_0 of the gas. Assuming , that the gas clusterizes to ~100% (which is nearly fulfilled in the experiment) than the number of atoms per cluster is

$$N_{clust} = \frac{n_0}{N_{at/clust}} \tag{8}$$

Since gas density n_0 scales linearly with the backing pressure (6) it holds for the scattered signal:

$$I_S \sim p_0^3 \tag{9}$$

That means, in order to determine the cluster size one has to measure the scattered signal in dependence on the backing pressure !
In principle also an absolute determination of cluster size with aid of Rayleigh scattering is possible. Assuming the scattered signal is vertically polarized and the signal is detected in a

plane orthogonally to the polarisation direction, then the scattered signal in the space angle dΩ is in this special case given by [11]:

$$\frac{I_S}{d\Omega} = I_0 N_{clust} \frac{9\pi^2 V_{clust}^2}{R^2 \lambda^4} \left(\frac{n^2 - 1}{n^2 + 2} \right)^2 \tag{10}$$

with R- distance detector-scattering source. Here it is assumed that clustering is 100% and all clusters are of same size. To evaluate the number of atoms per cluster additionally follow relations are to be used:

$$N_{clust} = \frac{V_{streu} \cdot \rho_{gas} \cdot N_A}{N_{at/clust} \cdot m_{mol}} \tag{11}$$

$$V_{clust} = \frac{N_{at/clust} \cdot m_{mol}}{\rho_{fl} \cdot N_A} \tag{12}$$

V_{streu}- scattering volume, rgas- density of the Xe- gas, N_A- Avogadro constant, m_{mol}- mol-mass of Xe and ρ_{fl}- density of liquid Xe is assumed as density in the cluster. Inserting these equations into (10) and solving for $N_{at/clust}$ results in

$$N_{at/clust} = \frac{I_S / I_0}{d\Omega} \cdot \left[\frac{9\pi^2}{R^2 \lambda^4} \left(\frac{n^2 - 1}{n^2 + 2} \right)^2 \frac{V_{streu} \cdot \rho_{gas} \cdot m_{mol}}{\rho_{fl}^2 \cdot N_A} \right]^{-1} \tag{13}$$

An evaluation of the cluster size requires a measurement of both the intensity of the scattered signal I_s and of the incident signal I_0. Uncertainties may come from the scattering volume and the refraction index of the cluster. Additionally it is not taken into account the in principle also clusters with different size could exist. Therefore the accuracy of the cluster size determination is not very high and should be possible only within a range of one order of magnitude.
A proof of the applicability of the Rayleigh scattering model is to measure the angular dependence of the scattered signal I_s: in the case of the Rayleigh scattering the signal is isotropic,while for the Mie scattering it shows a maximum in the forward direction!
As it is seen in Figure 3a the measured scattering signalis nearly isotropic and therefore it is legitime to apply the Rayleigh scattering model for the evaluation of the cluster size.

In the following we describe the experimental procedure to evaluate the cluster size under our real conditions. Because the actual values may be influenced by further specifics [7], which are not included in Hagenas formulas, the presence of clusters in the gas jet was analyzed with a Rayleigh scattering technique [9]. The Rayleigh scattering cross section is as shown above proportional to λ^4 and thus the cluster gas jet was probed by a doubled laser frequency 2w0 (400 nm) beam having a pulse energy of 100 mJ and a pulse width of 200 ps. The beam diameter was 1.5 mm. In order to reduce the background of unwanted scattered light the entrance and the exit windows of the chamber, which are passed by the diagnostic beam, are mounted with two additional tubes at a distance of 2 m from the gas jet. The light scattered by the clusters was collected with a 2.5 mm diameter aperture of a glass fiber cable looking at 90

degrees with respect to the diagnostic beam axis. The scattered photons were registered with a photomultiplier tube (Hamamatsu R928) and additionally for some backing pressures in absolute terms using a cooled CCD–camera with known quantum efficiency. In order to exclude shot-to-shot laser energy fluctuation the (scattered light)/(incident laser light) relation was measured. Fig.3 shows the scattered light signal as a function of backing pressure. Scattered signals above the noise level were observed starting from 5 bar and they are increasing nonlinearly with backing pressure. In some work where nozzles with large

expansion angles have been applied the observed scattered signals S scaled with backing pressure p_0 as $S \sim p_0^3$ [12]. Our measurements between 5 and 55 bar indicate that the scattered signal scales with backing pressure as $\sim p_0^{2.5}$ that gives an exponent somewhat lower than in [7].

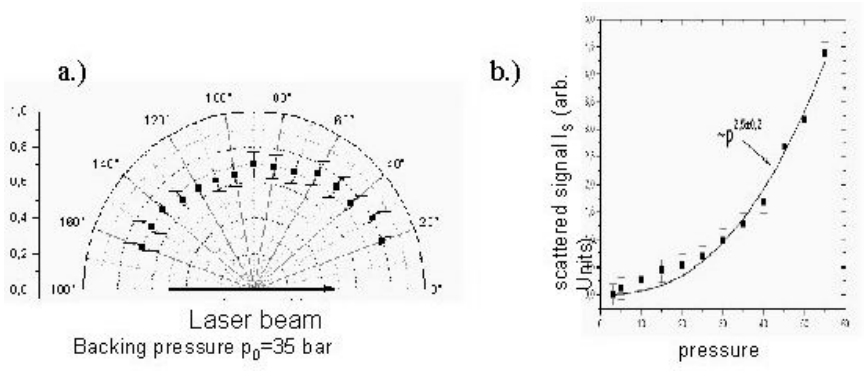

Figure 3: a.) Angular dependence of the scattered signal. There is up to p_0= 35 bar a nearly isotropic angular dependence of the scattered signal. The Rayleigh-scattering is dominant - no Mie- scattering.b.) Nonlinear signal grow: Clusterization takes place and the size scales with pressure.The exp 2.5 instead of exp 3 can be explained with the assumption that not all clusters have the same size.

This deviation prompted us to compare predicted values by Hagenas formula with an absolute cluster size determination. In general one meets several difficulties in order to access all parameters which determine the absolute size of the scattering signal (see [9] and [13, 14]). We determined at some backing pressures scattered photon numbers in absolute terms. The decrease of the average density in a nozzle flow [7] was used, which gives the number of atoms in the scattering volume if its appropriate size is taken. Therefore our estimations are subjected to relatively large uncertainties. A quantitative estimation of the cluster size based on scattered photon numbers and assumtion of 100% condensation into clusters gives a linear relation between cluster number and backing pressure. Our measurements confirm this dependence as the scattered signal S indicates the cluster sizes between $(3–10)\times10^5$ atoms at 5 bar and $(2–8)\times10^6$ atoms at 50 bar of the backing pressure.
A stable creation of large clusters has to be supported by an efficient source, i.e. it requires also an optical thick target. The latter is a pre-requisite for good laser light absorption and efficient ionization at short wavelengths emission of desired ionic species. The absorption behaviour was determined by a measurement of the laser energy transmitted through the target as a function of the backing pressure. However, this method implies a low level of scattering and reflection of the high intensity laser beam. Several work [15-19] have relied on this. Zweiback et al. [19] measured negligible and below 1% scattered intensity in both forward- and backscatters for targets containing large clusters (up to 6×10^5 atoms/cluster).Therefore the transmitted energy of the driving laser through the cluster target can be related to the absorption characteristic. In case of our measurement we make also use of the detector. Because the entrance pinhole (50 mm diameter) of the spectrograph is aligned along the laser beam axis some laser light penetrating through the 200 nm Zr–filter (few percent transmission at 800 nm) and diffracted by the pinhole can be detected on the CCD in the surrounding of the zero order of the grating spectrometer. This illuminated area is clearly distinguishable from the EUV–spectral traces and can be used to derive a signal which scales linearly with the laser light signal having passed the target and impinges to the entrance of the spectrograph. The in such a way obtained laser light transmission curve (Fig.4) shows, that the cluster target can really form a dense object for powerful optical femtosecond laser pulses [14,15] and already at low pressures a sharp decrease in the transmission is evident. The drop

in transmission as discussed above is mainly due to enhanced laser light absorption because back and side scattering seems to be not predominant [19]. The obtained characteristics will be related to the EUV–emission results which are discussed in the next paragraph. The visible small maximum between 10 bar to 25 bar in the transmission curve was reproducible and probably not a bare valve characteristic. Its origin was not investigated further because no special x–ray signal variation has been found in relation to it.

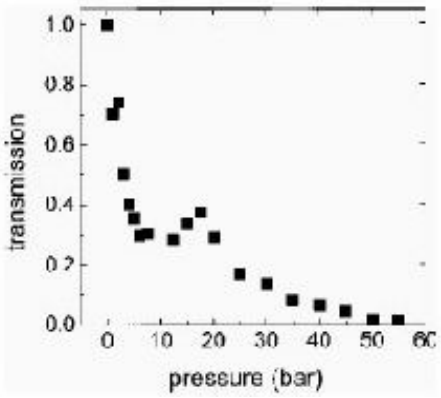

Figure 4: Measured transmission of the 50 fs, 800 nm Ti:Sa laser, focused at ~2×10^{18} W/cm^2 in to the Xe-cluster target in dependence from Xe backing pressure.

WP 2

Comprehensive measurements on the plasma parameters and spectral emission of Xe-clusters created under different conditions. These conditions are determined by the cluster dimensions, laser wavelengrth, laser pulse length, intensity and polarisation. The spectral range of the emission includes both soft X-ray emission between 10 and 15 nm and the resonance lines below 4 nm.

EUV - yield in dependence on the target characteristics

In Fig. 5 we depict spectra from the on-axis spectrometer obtained with different backing pressures. Three broadband emission peaks were observed in the 1 nm to 16 nm wavelengths range. The emission between 10.5 nm and 16 nm is well known from literature [21-23]. Four emission peaks were observed in this region which come from Xe^{9+} to Xe^{11+} ions. Most of the intensive EUV–emission occurs at certain Xenon ion stages and relates generally to transitions from resonance levels to the ground state of the respective ion. The emission region from (6-9) nm ((206-138) eV) has been observed in some spectral measurements [21, 22], but it was not addressed in further discussions. Taking into account that a typical relation between the energy of main contributing resonance states and the ionization energy is ~ ½ [20], Xe (XV – XVII) and higher ion stages can have strong contributions in this emission region. Between 6 nm and 7 nm the recorded signal decreases due to the transmission characteristic of the Zr–filter. Strong emission in the 1 nm to 2 nm wavelength region (Xe XXVII to Xe XXX) [24] was observed too (see Fig. 5) but not investigated further in this project (see Fig.5 and explanation in the text).

.

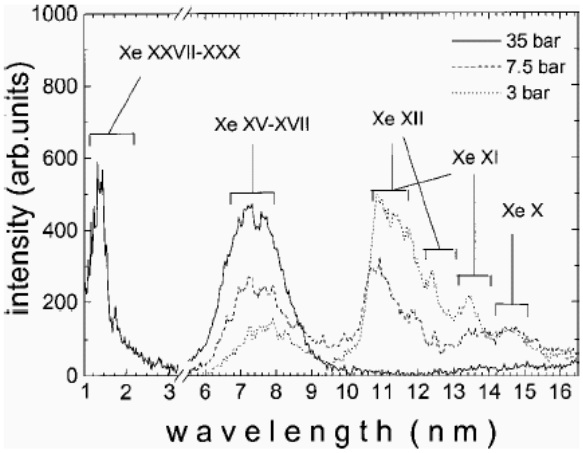

Figure 5: Spectra at 3, 7.5 and 35 bar Xe backing pressure registered with the on-axis TGS 2 and marks of emission line bands from different Xe ion stages. Emission between 1 nm and 2 nm is not shown for low pressure values because of an apparent optical background signal

A strong influence of the backing pressure and related target characteristics on the shape of the spectrum is already visible in Fig. 5. We investigated this behavior in detail and put a typical collection of spectra into Fig. 6. The full line represents the signal from the on-axis TGS (6nm–14nm) and the dotted one from the 45° off-axis TGS2 (10nm–14nm) which is absolutely calibrated in this range. With the help of a special cross calibration experiment where both spectrometers looked at the same angle to the radiating plasma object we can infer absolute photon numbers also from the second TGS. The signals below 10 nm refer to a relative scale in Fig.5. Starting from 1 bar we found an optimum pressure for maximized emission around 11 nm and 13 nm. The maximum yield in on–axis emission was registered at 3 bar and that in 135° off–axis direction at 15 bar backing pressure. A further pressure increase lead to a continuous drop of the 11 nm to 13 nm emission band up to a vanishing signal in on-axis direction while in off-axis direction this spectral signal keeps visible at a 3 ¸ 4 times reduced level. On the other hand we observed a continuous increase of the (6 - 9) nm band with increasing pressure up to 35 bar and a slightly following decrease up to 55 bar pressure. This part of spectra was only measured with the lower dispersive TGS in on–axis direction because we paid more comparative attention to the 13 nm region in this series of experiments. For intense laser pulse interaction with gaseous targets containing large atomic clusters a formation of high density plasma "balls" is anticipated which leads to an efficient laser energy absorption (cf. Fig. 6). Furthermore in analogy to plasmas produced from solid state targets high ionization states can be produced via collisions before expansion disassembles the small plasma cluster ball. After expansion the properties of our plasma will be similar to a low density plasma. In case of our relevant cluster sizes hydrodynamic expansion is predominant and the cluster expansion time t_{exp} is approximately [25]

$$\tau_{exp} \approx r_c \, (m_i/(Z\, kT_e))^{1/2} \, (n_c/n_s)^{1/3} \qquad (14)$$

where r_c, n_c is the initial cluster radius and density, respectively, n_s is the surrounding average gas density, kT_e is the cluster electron temperature and Z is the average charge per ion with a mass m_i in the cluster.

In case of a Xe–cluster with a 40 nm diameter (~ 10^6 atoms/cluster) and heated to an initial electron temperature of kT_e = 1000 eV [22] one obtains an expansion time of ~ 6 ps. In general one can conclude that increased cluster size increases the laser light absorption because the ions in the cluster hold together for a longer time and favoring thus energy transfer processes which act efficiently at high electron and ion densities.

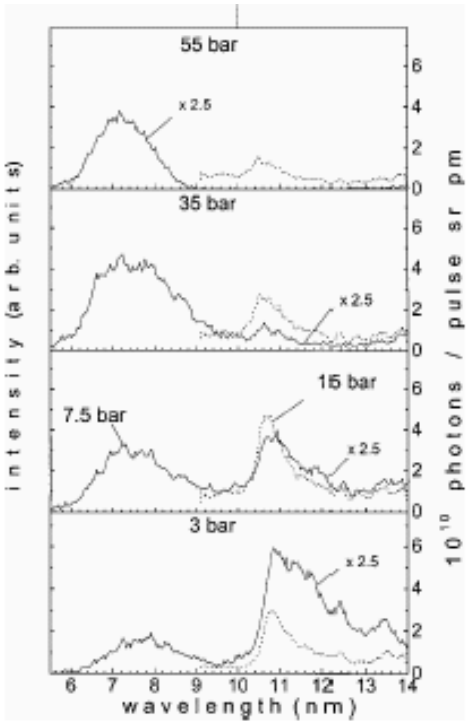

Figure 6: On-axis (solid line) and off-axis (dotted line) spectra with absolute photon numbers (right axis) for wavelengths above 10 nm at relevant Xe backing pressures. (On-axis spectra have been scaled down for better comparison). Values below 10 nm (dashed division line) refer to the relative intensity scale (left axis).

At already low pressures with the onset of cluster formation a sharp decrease in the transmission of the heating laser beam through the cluster target occurs as seen in Fig.4. This fits well growing cluster size as it is manifested in Fig.3 from the Rayleigh scattering experiments. The collection of our spectra in Fig.5 and Fig.6 shows the emission characteristics of our target as a function of the backing pressure. Qualitative changes in the spectra are observed with both our spectrometers, the on–axis and off–axis one. But the pressure ranges where maximum and minimum emission occur are different. In case of the on–axis spectrometer the emission signal between 11nm and 13nm is very low at pressures above 30bar. In contrast to lower pressures the maximum on-axis signal is 2-3 times higher compared to the maximum signal from the off–axis spectrometer. Although we cannot give a detailed solution on this question we want to make some arguments and simple calculations which could count for this differing behavior.
Our gas–cluster target has an extension of approximately 1.4mm (orifice diameter). Inside we produce the heated plasma emission source. If we relate the focusing conditions (confocal length $2\pi w_0^2/\lambda$, diameter $2w_0$) to the extensions of the produced plasma object, the spectrometers look to an object, which has probably a much shorter (10 ¸ 20 times) transverse dimension compared to its main axis (≡ laser axis) (similar to source pictures in [16]). Because the observation solid angles of the spectrometers are large enough one would not expect different signals due to the detection geometry.Registered signals may be influenced if absorption comes significantly into play. Based on Hagenas scaling laws [6,7] we estimate a concentration drop of Xe to a 1 % level in the target region compared to the stagnation chamber. Thus high backing pressures (50bar) give average atom densities of xenon, which relate to already short absorption length. At 50bar and photon energies of 95eV to 115eV (10.8 nm to 13nm) the absorption length amounts to (30 ¸ 40)µm, at 177eV (7nm) the absorption length is 800µm [26].

Different registered signals can result if the radiation passes different length of the absorbing medium. In our target such a situation can occur if the radiation emitting plasma object is not placed in the center of the ambient cluster gas. Miura et al. [16] showed with a series of source images how an ultrafast laser (100fs pulse length, KrF–laser, focal intensity 8×10^{17} W/cm^2) forms a plasma in an extended Xe-cluster gas plume as a function of the backing pressure. At higher backing pressures, the laser absorption is stronger in the first part of the cluster gas plume which shortens the length of the plasma and moves it out of the center of the plume.
Because our laser and cluster gas parameters are not far from Miuras ones we set up a simple source model which is based qualitatively on the experimental findings of Miura. We regard only a one dimensional plasma column in a 1.4 mm diameter cluster gas plume. From [27] an exponential decrease of the plasma source length versus backing pressure and a respective source movement is approximated. At very low backing pressures a centered position of the plasma column is given. In view of the laser propagation the plasma start point is kept at a fixed position whereas the end point of the plasma column moves closer to the start with increasing density and cluster size.

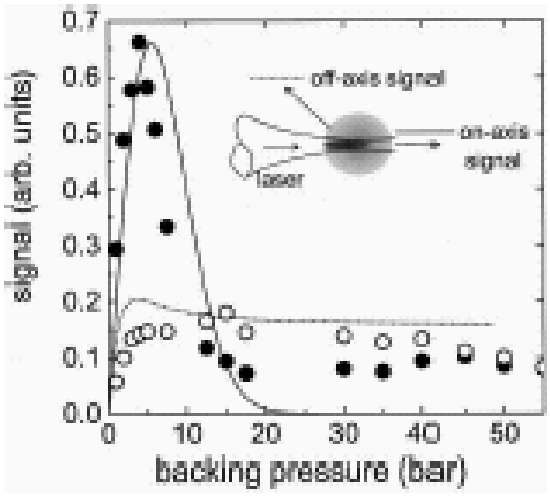

Figure 7: Registered on-axis (closed square) and off-axis (open square) emission data at 13.4nm in comparison to a computed signal (solid line – on-axis, dotted line – off-axis)

On the basis of a simple geometric target model which is supported by the experimental findings of [27] (details see in text), insert shows detection geometry. Our detection geometry is schematically depicted in the insert of Fig. 7. The signal of the plasma source is scaled linearly with the average atom density and the absorption [24] of the ambient cluster gas is calculated in dependence of the viewing angle of each source point. Because of inadequate knowledge of the EUV–absorption in the ionized plasma it is set to zero. In Fig. 7 we depict the registered emission at 13.4 nm versus backing pressure together with a function plot of our simple target model. Both curves are fitted together in dependence on one parameter for the signal height and one for the source extension. From Fig. 7 it is visible that the general behavior of signal increase and decrease can be reflected with the simple model, which of course can not account for all the details of the experiment.

EUV–yield in dependence on the laser polarization

Several experiments (see [15,28]) have revealed that collisional processes can play an important role for cluster heating resulting in the release of highly energetic ions up to MeV energies and hard x-ray emission. Therefore it is of interest to what extend collisional heating of the electrons by inverse bremsstrahlung and stimulated Raman scattering [25] influence the ion species being responsible for the EUV–emission looked at this work in the frame of the project.

Before collisional heating of the laser plasma can occur an initial ionization of the system has to take place. Optical field ionization is the relevant process if high intensity ($>10^{15}$W/cm^2) ultrashort laser pulses are applied. For our focal intensity of~ 2×10^{18}W/cm^2 it is obvious that ionization rates [29] from Xe to Xe XII are several orders of magnitude higher than an estimated maximum collisional ionization rate from Xe X to Xe XII which is in a range of 10^9 -10^{10}s^{-1} [30]. Indeed the laser intensity applied here is capable to produce ions up to Xe XXVI. Therefore it is worthwhile to think about a change of the laser parameters in such a way that the laser field and the following tunneling process directly influence the spectrum of the initially ionized electrons. This can be done by changing the laser polarization from linear to circular [31]. The experiment may show whether this change is visible or ´´washed out´´ by following collisions. From theoretical considerations, however, EUV spectra generated with linearly and elliptically polarized laser light should show a significant difference due to resulting higher energies of electrons field-ionized with circularly polarized light [32-34]. Up to now experiments have verified this mechanism in low density gas targets [32], where other heating mechanisms are ineffective. Contrary to this in case of high density gas jets or in cluster targets the initial field ionization is thought to be followed by further collisional processes which in turn modify the ionic state distribution. Furthermore defocusing arises from a refractive index gradient which is caused by an ionization variation across the beam [33] and that makes the picture more complicated. Because of these difficulties no conclusions could be drawn how sensitive the polarization influences the ionization of a large Xe–cluster target and the related EUV–yield. Therefore we proceed with a polarization dependent excitation experiment which was not reported so far for Xe–clusters.

Circularly polarized laser light was produced by inserting a λ/4–plate in the beam. An obvious difference in the emission yield using the two different polarization states was detected with the off-axis spectrometer as depicted in Fig.8. In the whole range of relevant Xe backing pressures the emission around 13.4nm is about 2 times higher if circularly instead of linearly polarized light is used. At 10bar the ratio is about three times. The same feature was registered for the (10-15) nm emission band in off-axis direction. In Fig.9 emission data at 13.4nm, 11.4nm and 7.5nm from the on-axis spectrometer are collected. At 11.4nm and 13.4 nm there is still some enhancement with the circular polarization visible, but it is only a factor between 1.1 and 1.2 at peak signal. Once more, similar to the discussion concerning Fig. 7, the peak signal level detected with the on-axis spectrometer is up to 2 -3 times higher compared to the pressure optimized value for the off-axis one. From our experimental findings we can thus conclude that the emission signature in the 10nm to 15nm wavelength region is not totally determined by collisional processes. The influence of the initial field ionization is visible and a change in laser polarization can be used for EUV–yield optimization.

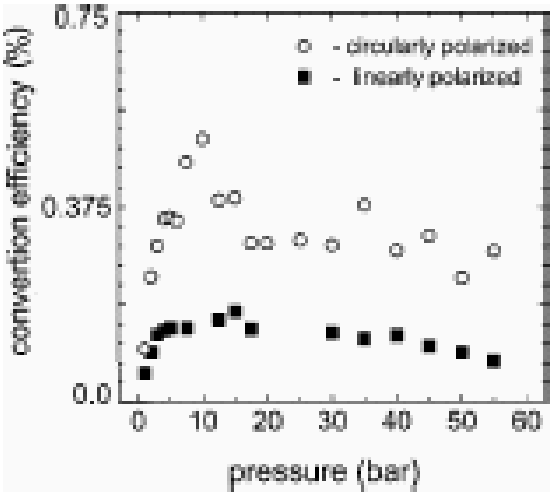

Figure 8: Conversion efficiency at 13.4 nm related to recorded off-axis EUV-emission and incident laser energy E_L at different Xe backing pressure when linearly (E_L= 180 mJ) and circularly (E_L= 75 mJ) polarized 800 nm laser light is used for excitation. Change in laser energy was due to operational reasons. In this range the conversion efficiency does not change at constant polarization.

Table 2. Conversion efficiency as function of pulse duration and polarizaion of the laser pulse

Pulse duration, polarization	Conversion efficiency % in 2psr 2.2%bw	Xe pressure bar
50 fs, linear	0.2	15
2 ps, linear	0.2	20
50 fs, circular	0.5	10
2 ps, circular	0.8	15

In off–axis emission direction possible features may be also concealed by absorption in the plasma regarding the signals at 11 nm and 13.4 nm. (For simplicity this has been excluded in the simple target model discussed above but it may be a too crude assumption for explaining all the data). At 7.5 nm the absorption in the ambient gas is much weaker and the emission is observed up to maximum pressure in off–axis direction (on–axis the spectrometer cuts at 10 nm). The 7.5 nm signal in Fig. 9 shows no clear dependence from polarization. Here the emission is already carried by higher Xe–ionization stages, which suffer probably a stronger influence by collisional processes, which ´´washes out´´ the initial ionization imprint. Collisional excitation of higher ionization stages becomes important after initial ionization due to high energy electrons (the rate coefficients for collisional ionization becomes higher with increasing electron temperature [30]). Recently Kumarappan et al. [35] found that the Ka–emission in the keV-range from Ar-clusters does not vary with the laser polarization, which would support the observed trend by us. The signal variation in Fig. 9 (bottom) we would not attribute to simple data fluctuation covering a range of about 20 % but its origin keeps unrevealed in this work. With increasing pressure and growing cluster size collisions favor the production of higher ionized states and thus the emission center of gravity can be shifted to shorter wavelength. This effect could not be detected conclusively in our limited

wavelength range of observation and possible indications may be covered by EUV–absorption as discussed above.

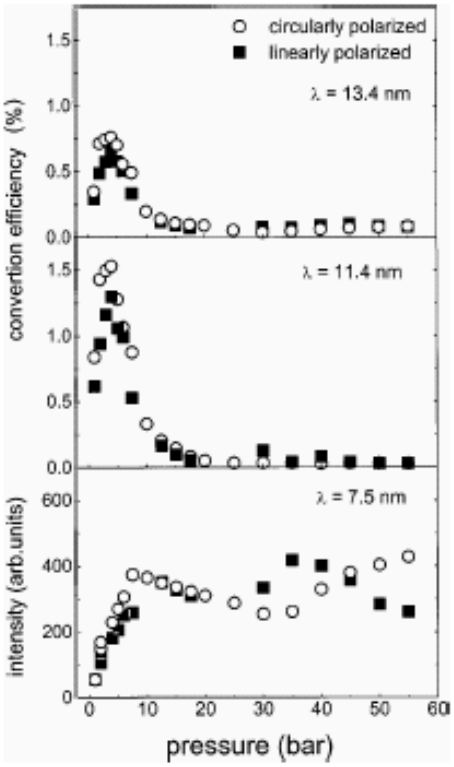

Figure 9: Observed on-axis conversion efficiency for 13.4nm, 11.4nm and relative intensity for 7.5nm from Xe-cluster targets at different laser polarizations.

Conversion efficiencies as function of the pulse duration

Now results are introduced on the examination of the interaction of ps- up to ns- laser pulses with the large Xe clusters. One surprising result is that a 10 ns laser pulse with an intensity of 10^{14}W/cm^2 can produce an EUV emission (13.4nm) with a comparable conversion efficiency of 0.26% in 2π steradian (sr) and 2.2% bandwidth (BW) as it was recorded for a 30ps laser pulse with an intensity of at least 10^{15}W/cm^2. Whereas the conversion efficiency allows to estimate EUV photon number per laser pulse, dependence on laser repetition rate determines the maximum irradiation frequency for the target and thus will give us information about the average flux, which, as mentioned earlier, has important implication for potential applications.

The experiments were carried out with our Nd-YLF burst laser system (λ= 1047nm) described in [36]. This laser provides an average power per burst up to 5kW corresponding to 4J total burst energy. The length of the burst was 800μs. The number of single laser pulses per burst can be adjusted from 25 to 800 per burst, i.e. repetition rates up to a maximum of 1000kHz are possible. In our experiments we used single pulse durations of 30ps, 300ps and 3000ps. By changing of the laser energy an intensity range between 10^{11}-10^{15}W/cm^2 could be covered.

Soft X-ray and EUV spectra from the Xe-cluster target were measured at fixed laser energy of 2.4J per burst (with 100 pulses per burst) under an angle of 135° to the laser beam backward direction (TGS-1) and along the laser beam axis (TGS-2). The pulse duration was varied between 30 ps and 3 ns. The nozzle backing pressure was 30-40bar. While the TGS-1 recorded the EUV-emission in the 10-15nm wavelengths range (Fig.10b), the TGS-2 covered the emission in the whole wavelength region from 1-16nm (Fig.10a).

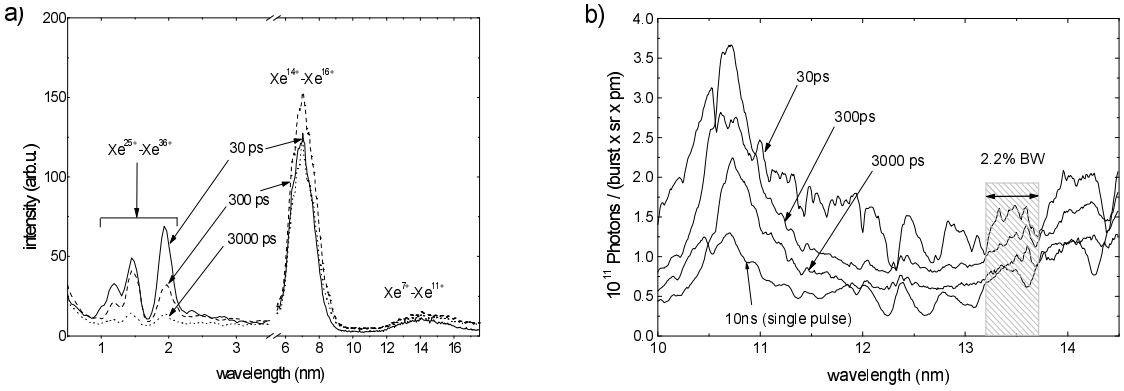

Figure 10: X-ray (a) and EUV (b) emission spectra of a Xe plasma measured correspondingly with TGS-2 and TGS-1 spectrographs at 30, 300 and 3000 ps laser pulse duration with intensity of 1×10^{15} W/cm^2, 1×10^{14} W/cm^2 and 1×10^{13} W/cm^2, respectively.

In Fig. 10a three emission bands can be clearly recognized, one at 1.85nm, another at 1.4nm and a third one at 1.2 nm. In a theoretical model describing the highly-resolved spectrum of the emission around 1.85 nm [37], generated at similar laser irradiation conditions as in our experiment, it was shown that strong dielectric recombination of 25-27 times ionized xenon can efficiently contribute to the emission in the cooling phase of the plasma. Characteristics of X-ray emission in the 1.25-1.6nm range from a Xe clusters target irradiated by 2ps laser pulses at intensities near 10^{17}W/cm^2 were investigated in [38].
The authors of [9] stated that a signal could be measured only in case of irradiation with a short wavelength KrF (248nm) laser instead of Ti:Sa (800nm) laser with comparable intensities. In contrast to that short wavelength high-intensity irradiation experiment we have seen the emission between 1-2nm well pronounced also at much lower laser intensities and even at ns-laser pulses. Moreover, whereas in [9] the relative intensities of the 1.2 and the 1.4 nm peaks are quite different in our spectra the difference is only of a factor of ~ 2. In Fig.10b it is visualized how the emission spectrum varies with laser intensity at the three different pulse durations of 30 ps, 300 ps The emission in the region between 0.8-1.6 nm excited by 350fs laser pulses at intensities (4-8) $\times10^{17}$W/cm^2 was reported in [24]. The third emission band around 1.2nm was only slightly visible in X-ray spectra shown in Fig.3 in [24]. The authors stated there that a signal could be measured only in case of irradiation with a short wavelength KrF (248 nm) laser instead of Ti:Sa (800 nm) laser with comparable intensities. In contrast to that short wavelength high-intensity irradiation experiment we have seen the emission between 1-2 nm well pronounced also at much lower laser intensities and even at ns-laser pulses. Moreover, whereas in [24] the relative intensities of the 1.2 and the 1.4 nm peaks are quite different in our spectra the difference is only of a factor of ~ 2. In Fig.10b it is visualized how the emission spectrum varies with laser intensity at the three different pulse

durations of 30 ps, 300 ps and 3000 ps at the same laser energy. Although the laser intensity at the three different pulse duration drops down by a factor of 10 one could see a considerable change in a wavelength region of 1-2nm only when a 3ns pulse and lowest laser intensity was used. The measured strong emission from the highly charged Xe-ions (up to Xe^{+36} ions (see also [18])) is also likely caused by the highly efficient laser energy deposition in the cluster target. It should be noted that we could not investigate the wavelength region between 3 - 6 nm due to high absorption of the used Zr-filter in this emission region.

However, to make a decision whether a Xe-cluster jet could be a favored target system its capability to convert laser energy in to the 13.4nm emission must be investigated in dependence on laser pulse duration as well as repetition rate. For the evaluation of the conversion efficiency we analyzed the spectra from the TGS-1 spectrometer in the bandwidth (BW) of 2.2 % around the 13.4nm signal emitted into a solid angle of 2π steradian. The measurements showed that at different laser pulse duration the efficiency depends on the source pressure, respectively cluster size. Therefore the evaluation was made using the signals for optimum pressure. These parameters were 30bar at 30ps, 40bar at 300ps and at 3000ps pulse duration (see Figure 12a). The results of the measured efficiency in dependence on the laser intensity and pulse duration are shown in Fig.11. It is expected that the efficiency should have an optimum depending on the laser pulse intensity as observed with a water jet target [39]. However, in our case the efficiency increases still continuously with the laser intensity.

Obviously, the intensity of a single pulse in the burst was not high enough to cover the optimum range. As one can easily recognize in the case of comparable intensities longer pulses are producing higher conversion efficiency. Whereas it is not so well pronounced for 30ps and 300ps pulse durations, for pulses with 300ps and 3000ps the longer pulses clearly create higher conversion efficiency. Therefore we used an 10 Hz Nd:YAG laser with maximum pulse energy of 0.975J and a pulse duration of 10ns in order to examine the intensity scaling of the efficiency for longer pulses. The laser beam was focused to an intensity of almost $10^{14}W/cm^2$ in the same 10μm spot size (FWHM) as the burst mode laser. Although the Nd:YAG laser parameters are very different from that of the burst mode laser, the efficiency for the 13.4nm emission was 0.26% in 2π steradian and 2.2 %BW, which fits well in the intensity scaling derived from the burst mode laser (Fig.11). In the parameter range covered here a higher pulse intensity results in still higher efficiency. However for the long 10 ns pulse duration the maximum efficiency is larger than the best one achieved with the burst mode laser but at the one order of magnitude higher intensity. It is worth to note that the measured efficiency was in the range of the highest values reported in the literature using Xe-cluster or Xe-gas target system and laser pulses with moderate intensities [27,40,41]. The influence of laser pulse duration on Xe-plasma production and related EUV-emission can be discussed in context with the plasma expansion time [42]. Inside the cluster media laser energy can be effectively absorbed if pulses are shorter or comparable to the disassembly time of the clusters. This is just in the range of few picoseconds [25,42]. When using laser pulses in the ps-range the Xe-plasma creation and related EUV-emission depend on the initial cluster state of the target. Thus we put emphasis on cluster target characterization and optimisation too. In case of laser pulses with ns-width only the leading edge of the pulse can interact with a cluster. Later on the cluster disassembles and the resulting underdense uniform plasma will determine the plasma dynamics. A complete understanding of the observed differences in ps- and ns-pulse interaction (cf. Fig.11) cannot be obtained without a modelling of the complex

a.) b.)

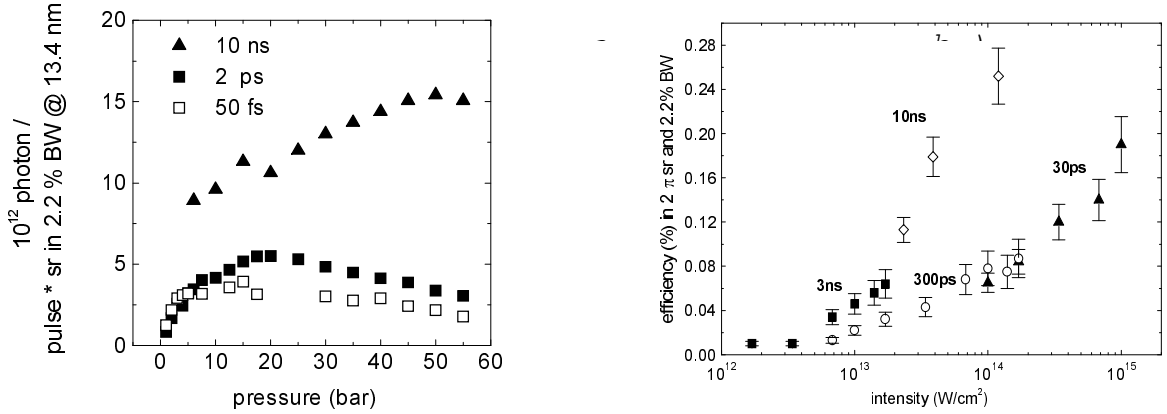

Figure 11.a.) Conversion efficiency at 13.4nm wavelength in dependence of the laser intensity at pulse durations: The evaluation was made using the signals for optimum pressure. These parameters were 30bar at 30ps (triangles), 40bar at 300ps (circles), 3000ps (squares) and 10ns (diamonds) pulse duration. b.) Emitted photon number (off-axis) at 13.4 nm in dependence of Xe backing pressure and different laser pulse widths and laser energies.

energy transfer processes in the target. However here we suggest how the EUV emission characteristics can be understood in an empirical picture of the plasma dynamics where the main part of the laser energy is transferred to that underdense uniform plasma. This may provide a simple model to explain, at least partially, the observed large difference in the conversion efficiency for 13.4 nm emission at different laser pulse width. Because of both the big clusters and the moderate laser intensity the target will be ionized during the leading edge of the laser pulse, but the plasma does not rarify at ns time scale and therefore laser energy can be efficiently absorbed. The first part of an ns-pulse could prepare a plasma state which provides a more efficient excitation for the following part even at reduced density. This is similar to the well-known plasma preparation by different prepulse techniques for optimum excitation.

In [43] the authors reported that the prepulse technique applied to a 10bar backed Xe gas jet has got a 2.5 fold emission enhancement at about a time delay of 100ns. For the further discussion we try to approximate the plasma density evolution of the source when the source size is in the order of 600mm. (The source size was measured to be significantly larger as the laser focus extension. Perpendicular to the laser propagation axis we measured a source extension of about 600mm. We also could not observe any size effects in dependence on the pulse duration). From our spectral measurements (different line radiation from different charge states as discussed above) we can assume to have an average charge state Z_{av} in the order of 10 for the radiating Xe-plasma.

This averaged ionization of Xe is approximately related to an electron temperature kT_e in a range between 50 eV and 100 eV. The thermal plasma expansion velocity v_{pl} can be estimated from

$$v_{pl} \approx (Z_{av}\ kT_e/m_{ion})^{0.5} \qquad (19)$$

and reaches here a value of $v_{pl} >> 2\text{-}4\times10^6$ cm/s which is not very high due to the massive Xe-ions. If we now look at the plasma density evolution approximated by

$$n_{pl}(t) = n_{pl}(0)\frac{1}{(r_0 + V_{pl}\,t)^3} \qquad (20)$$

and having used an initial radius r_0 of 300μm the expanded radius after 3 ns will be 360-450 μm and the average plasma density decreases by a factor of ~1.7-3. The initial plasma density corresponds to the average Xe-density provided by our target system. It is to n_e~ (3-4) $\times 10^{19}$cm^{-3} at 30–40bar [7] and fits well the data extrapolated from [41]. Within this picture the density remains nearly constant in the first 100 ps and decreases slowly in the following 10ns. Thus it seems to be reasonable that for 30ps and 300ps pulses but with comparable intensities of ~ 10^{14}W/cm^2 the conversion efficiency at 13.4nm are similar (Fig.12). At the available density level of n_e=4×10^{19}cm^{-3} one can estimate a possible laser radiation absorption via electron-ion collisions [41]. The absorption coefficient is

$$\alpha_{abs} = \frac{\nu_{ei}}{c}\left(\frac{\omega_p}{\omega_L}\right)^2\left(1-\left(\frac{\omega_p}{\omega_L}\right)^2\right)^{-0.5} \qquad (21)$$

with ω_p- the plasma and ω_L- the laser frequency, respectively. The electron-ion collision frequency is

$$\nu_{ei} = 2.9\times10^{-6}\,\frac{Z_{av}^2\, n_i\left(cm^{-3}\right)\ln\Lambda}{T_e(ev)^{3/2}}[s^{-1}] \qquad (22)$$

[44] where the Coulomb logarithm is approximated by lnΛ=24-ln ((n_e[cm^{-3}])$^{0.5}$/T_e[eV]). For the absorption A=1-exp(-α_{abs} d) we obtain values between 3% and 22% for a source extension of 600μm and using ion density values n_i between (2-4)×10^{19}cm^{-3}, an electron temperature of 50eV and an average charge state 10. At least this rough estimation shows that efficient laser light absorption can occur for our target parameters during a relatively long ns-timescale. This is corroborated by the experimental findings in Fig.12 and by our previous investigations [45]. The ns-pulse interaction results in a higher conversion efficiency compared to ps-pulse interaction at an intensity level of 10^{14}W/cm^2. The obtained experimental results depicted in Fig.12 advise that the laser intensity plays the crucial role for the interaction efficiency with cluster-jet targets. Other experiments [46] found similar to us that the efficiency minimum when using ns-pulses at a 10^{12}W/cm^2-level. But here we could perform experiments at higher intensity. Thus probably a higher ionization occurs over a longer timescale, which boosts finally the EUV-emission efficiency. However we could not reach the intensity for an excitation optimum, neither for ns- nor ps-pulses. It should be remembered here that in a previous work [42, 47] we showed higher efficiencies, but for remarkably higher intensities in the range between 10^{16}–10^{18}W/cm^2 and with ps- and fs-laser pulses as described above..

The results implicate that cluster target heating on different time scales change the interaction type from the common cluster dynamics on a ps-timescale to a dense gas interaction characterized by a ns-timescale. The latter one can be effective on the precondition that sufficient average density and laser intensity will be provided. Effects, which could now increase the conversion efficiency within the discussed qualitative model of plasma expansion, can be connected either with a more efficient creation of the required ion species if the plasma can be heated over a longer timescale or with an efficient suppression of the quenching of the relevant excited states by three-body collisions due to the decrease of the

density during the expansion. This may provide a argumentation for the observed large difference in the conversion efficiency for 13.4nm emission at different laser pulse width.

Conversion efficiencies and comparison to other laser driven Xe–sources

Within a 2.2% bandwidth centered at 13.4nm, a wavelength band where Mo:Si-multilayer mirrors with highest reflectivity (~70%) can be provided, the total integrated off-axis flux in relation to the incident laser energy (conversion efficiency) is shown in Fig. 12. Here we extrapolated the emission in 2π sr solid angle using the observation angle of 0.05msr of the off-axis spectrometer. Averaging the off-axis and on-axis data we can infer a maximum laser light into EUV-emission conversion efficiency (CE) of 0.5% in 2π sr solid angle. At around 11.4nm in respect to Mo:Be multilayer mirrors with highest reflectivity the CE amounts to 2 % in in 2π sr solid angle (cf. Fig5). Moreover in the wavelength region from 10nm to 15nm a CE up to 7.5% in 2π sr has been achieved. Our data exceed the conversion efficiencies obtained in experiments where Xe cluster targets were irradiated by KrF laser pulses with 100 fs pulse length [16]. Conversion efficiencies of 1.1% in 2π sr at (11±0.27)nm and up to 7% in 2π sr in the region from 5nm to 20nm. have been reported. Some applications (e.g. lithography) require continuous or quasi continuous – high repetition rate – illumination where the single temporal pulse width does not and only the average power does matter. Therefore it is important to compare our conversion efficienies with efficiencies of other Xe–aggregations (e.g. liquid) in a different laser interaction parameter regime (ns-laser pulses). Our CE at 13.4nm is very similar to the related value given by D.A. Tichenor et al. [48] who has found for ns – irradiated Xe cluster/microdroplet-targets (cf. comment in [46]) a CE of about 0.7% in 2π sr and 2.2% bandwidth (BW). In contrast, for a Xe jet-target irradiated by YAG laser pulses of 10ns duration CE's were reported [49] of 0.6% in 2π sr and 0.2% in 2π sr at 11.4nm (1% BW) and 13.4nm (2% BW), respectively.

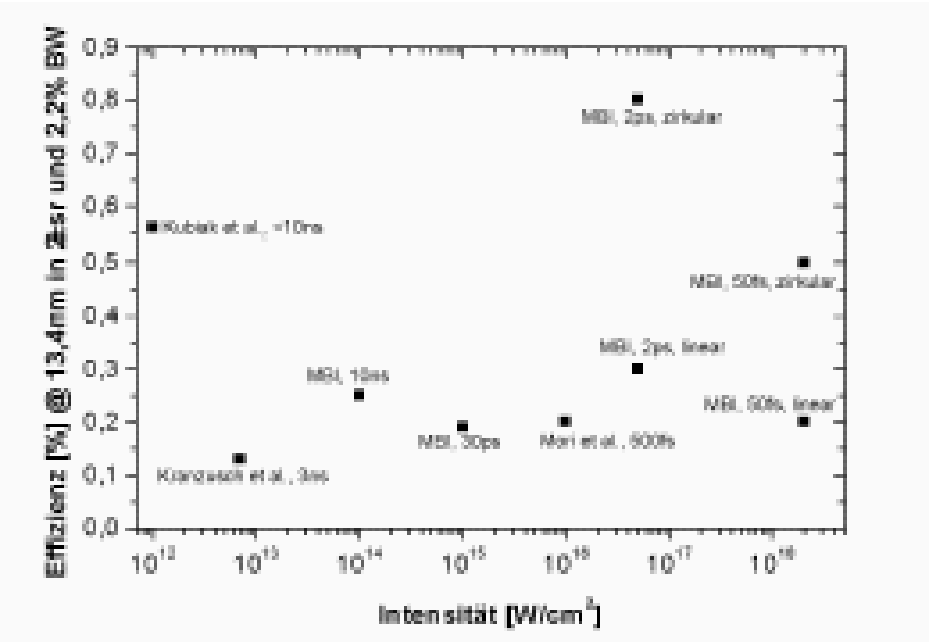

Figure 12: Comparison of published conversion efficiency values of Xe-gas-pulsed/cluster targets at the 13.4 nm wavelength

Finally, in the following an estimation of the efficiency will be made based on the assumption that the plasma is in an local thermodynamic equilibrium (LTE). In contrast to water, for the

Xe is the estimate of the required ionization energy difficult, because several different ion species contribute to the emission with a bandwidth of 2.2%because several different ion species contribute to the emission in the bandwidth of 2.2% at the 13.4nm wavelength. Moreover, the energy of all possible transitions contributing to the emission in this range are not known (not accessible !). Therefore following assumptions have been made:
The emission in the EUV range stems mainly from the Xe^{7+}-Xe^{11+} ion species. We take for the estimation of the efficiency an averaged ionization energy value for the Xe^{10+} $\sum E_t^{10} \approx 815eV$. Additionally it is presumed that the ten-fold Xe-ion emits mainly in the range between 10-15nm, which is covered by transmission grating spectrometer TGS 1. Now we can compare the radiated energy in the whole range with that from the 13.4nm in-band range. It follows from the comparison of the energy contained in the whole range to the in-band energy a value of $\sum_{j=a}^{\omega} \gamma_j h\nu \approx 1000eV$.
The ion and electron temperature is approximated to $k_B T_j \approx 60eV$. With all that physically justified approximations one receives an $E_{min} \approx 2800eV$ and respectively a theoretically possible conversion efficiency of $\eta \approx 3.5\%$ in 4πsr and 2.2% bandwidth or about 2% in 2πsr. These values for the conversion efficiency are in coincidence with other calculations reported in the literature [50]. They represent an upper limit since it is but not taken into account other factors as an imperfect laser pulse coupling to the plasma. It seems to be reasonable to proceed from the assumption that the maximal conversion efficiency should not surpass the value of 1%. The experimentally determined efficiency for irradiation with a circularly polarized laser pulse comes already close to this estimated value. An important problem at the optimization of the efficiency is obviously the absorption of the created EUV-emission in the plasma. A way out of this situation could be a substitution of the cluster/gas target by an Xe-jet target, which is indeed in progress. It is worth to underline, that a more exact calculation would require a sophisticated hydrodynamics and radiation propagation code, which was not available.
Large Xe–clusters (10^5-10^6 atoms per cluster) have been exposed with ultrashort (50fs) and high intensity $(2–4)\times10^{18}$W/cm^2 pulses from a Ti:Sa-laser. Scaling and absolute yield measurements of EUV–emission in a wavelength range between 7nm and 15nm in combination with cluster target characterization demonstrate the role of cluster size, average density and target configuration for yield optimization. Maximum emission in the 11nm to 13nm emission band has been found with backing pressures between 5 and 15 bar. The registered anisotropy of on-axis and off-axis emission suggests an important influence of the source size, ion distribution and radiation absorption within the ambient cluster gas. A simple model of a possible source geometry can explain main features of the observed signals. With the laser parameters used here Xe^{9+}-Xe^{11+}–ions are produced via optical field ionization and are probably not essentially covered by further collisions. Therefore the use of circularly polarized laser light results in enhancement of the radiation signals in comparison to linearly polarized light. An absolute emission efficiency up to 0.5% in 2π sr at about 13.4nm wavelength and 2.2% bandwidth was realized. With longer 30ps–10ns laser pulses at moderate intensities ($<10^{15}$ W/cm^2) could also be demonstrated an efficient conversion of the laser energy in to EUV-emission. For the Xe-plasma a high conversion efficiency of 0.2% (2π sr, 2.2% BW) in to 13.4nm radiation was measured at laser pulse duration of 30ps and an intensity of 10^{15}W/cm^2. It is especially important that in case of 10ns laser pulses at 10^{14} W/cm^2 a still higher conversion efficiency of 0.26% (2π sr, 2.2 % BW) could be reached. In general, the radiation efficiency rises with increasing intensity. It was shown that the Xe-cluster jet target having a high flow velocity is well suited for efficient EUV-emission with high repetition of up to 125 kHz. Both the high conversion efficiency and the high repetition rate make this type of Xe-target attractive for high average EUV-power sources. Based on

available laser technology, further technical and application requirements can be chosen for a suitable Xe–target system for bright EUV–radiation.

WP3

Xe-clusters confined in a capillary
Characteristics of a dense, temporally and spatially localized, optically thin LTE plasma with a cold core. The techniques applied in WP2 will be applied here to the plasma in a free space and Xe-clusters confined in a capillary. Some specific techniques from the investigations of an ionized high-Z material will be applied to obtain fine tuning of the transition energy within the 3d-shell.

The experiments to confine clusters in a capillary discharge in order to produce an elongated efficiently excited plasma tube, which could be of importance for increase in the efficiency of the incoherent laser plasma sources in the XUV range failed. Our attempts applying diagnostics for the cluster characterization as described in the WP1 have shown, that clusters will be already damaged on the way to the interaction region by interaction with the cold plasma existing in the capillary. This result seems to be of general character once it means that the cluster can be created in a stable and controlable way only in a free-streaming jet.

WP4

We are going to use Ag soft X-ray laser working at 13.9 nm in Ni-like ions and determine optical characteristics of ist output beam (dimensions, divergence, intensity distribution, coherence) and subsequently couple this beam to the X-ray optics. The energy of a few microjoules and peak intensity of 10^{10} W/cm^2 are expected. Thus, some quasi-coherent source would be available for some applications.

Realization of a transient collisional x-ray laser

Very recently in contrast to the common transient schemes with two pulses, a new modified transient scheme was demonstrated using only one shaped short pumping pulse. The pulse was deliberately shaped to meet the requirements for the creation of a preplasma and following rapid heating phase. This method takes the advantage that the plasma created in this way is more symmetrical and homogeneous. This effect resulted in saturated lasing in Ni-like Ag at 13.9m with only ~3J of pumping energy [51]. One of the specific features of this scheme is, that the optimum duration of the pump pulse (FWHM) is between 5-10ps. That means, the system can show a moderate transient behaviour. This has also been confirmed by EHYBRID-simulations. The temporal dependence of the gain of a Ni-like Ag XRL at 13.9nm for the pumping parameters: 20mJ in the 2 ns background and 2.6J in the 6 ps main part of the pulse is shown in Figure 13. It has been easily seen, that the gain is very high even after 20ps, which is in contrast to the common double pulse pumped transient schemes. The duration of the output pulse is expected to be of the same order of magnitude. This was confirmed in experiments [52]. These pump pulse parameters are moderate and close to those of commercially available laser systems with higher repetition rate. Therefore, short pulse table top X-ray lasers of reduced size and high repetition rate are now realistic.
The advantage of this shaped single pulse pumping is evident: high plasma homogeneity can be produced, in contrast to the common double pulse schemes, where an exact spatial

superimposing is required. This homogeneous plasma distribution is a prerequisite for a high amplification in low-pumped system allowing to drive the system into saturation. As a result the operation parameters of this saturated Ni-like Ag- x-ray laser are quite impressive: Pump energy - 3J on 7.8mm target length, pump pulse duration ~6ps (with pedestal of 20mJ in 1ns), gl>16-saturation, output energy ~3-5μJ, i.e. photon number per pulse - 10^{11}-10^{12}.The pump beam was focused down to a line of a length of ~7.8mm and a width of 80 μm by a combination of an off-axis parabola and a spherical mirror. The pulses irradiated massive flat silver slabs of 4mm and 6.7 mm in length, respectively. The focal line was longer than the target length to keep the energy density nearly constant over the whole target length avoiding the creation of cold plasma at the target ends.

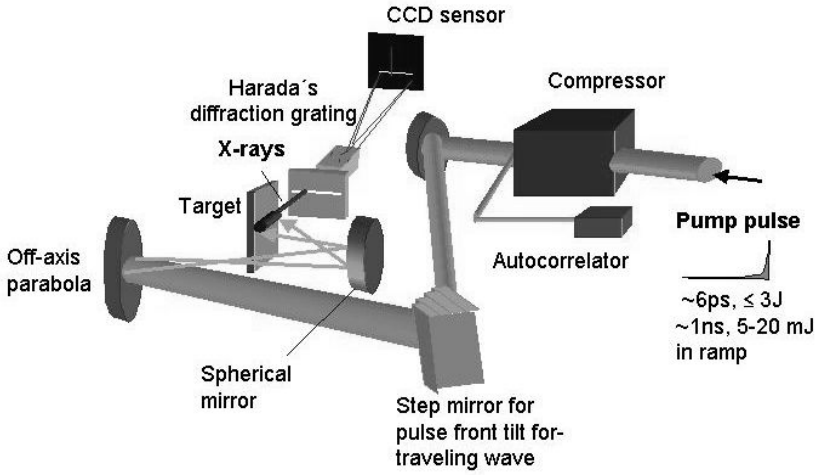

17

Figure 13: Scheme of a short pulse pumped hybrid capillary discharge XRL with a coupled soft x-ray flat-field spectrometer [51]. The inset shows the specifically shaped pump pulse

In Figure 14 the amplification behavior of this x-ray laser in dependence on the target length is given for the two cases- unmatched traveling wave velocity (full blue dots) and matched velocity (red spheres). As expected, the gl- factor is higher for the matched velocity, however somewhat smaller than it follows from calculations. This discrepancy is attributed to the relative long pulse duration of ~6ps and the steplike traveling wave arrangement. The full advantage of the traveling wave would would be apparent for shorter pump pulses and a continuous movement of the pump pulse along the focus line. Clearly visible is the roll-over of the gl-value at a target length of about 5mm, which can be understood as the transition into a saturated amplification.

However, inspite these notable results the propagation of the X-ray laser beam in the amplifying medium and the dependence of the x-ray laser beam quality (deflection, divergence, wavefront) on pump beam parameters is still not well investigated [53,54]. A better understanding of the transient collisional scheme can be gained from the measurement of the coherence of the x-ray output beam. Among the various methods to measure the spatial coherence of x-ray lasers, of particular interest is the usage of multi-slit arrays [49], double-slit gratings[56], knife edges [57], two-pinhole masks [58] or double-slits [59]. Increasing coherence with increasing gain length has been demonstrated for a neon-like Ar X-ray laser pumped by a capillary discharge [57,58].

In order to get more information about the propagation and amplification of the x-ray beam in the silver plasma column produced with our shaped single pulse technique we have looked more in detail for the spatial coherence properties of the Ni-like Ag x-ray laser at 13.9 nm. We use the method of Young's double-slit interferometry to measure the spatial coherence. The brightness of the transient x-ray laser is high enough to produce fringes with an excellent contrast in a single shot. The interferograms observed here are the first ever produced for a transient collisional excited x-ray laser pumped by a single picosecond laser pulse. We believe the compactness of the laser driver and the 13.9nm wavelength of the x-ray radiation, close to the optimum of the XUV reflective optics now available, makes such system particularly attractive for applications.

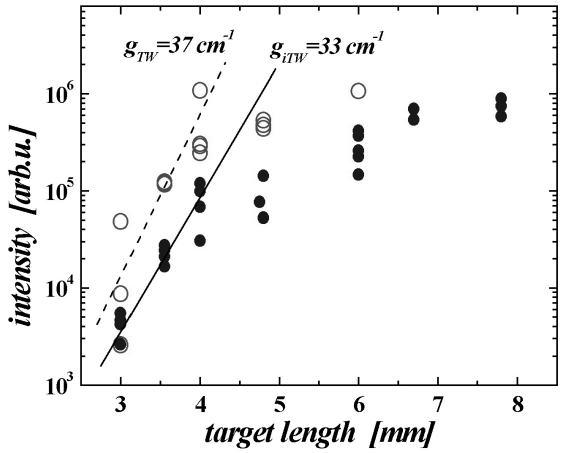

Figure.14: Amplification (gl-value) of the nickel-like silver x-ray laser at 13.8 nm for an unmatched traveling wave pumping (blue dots) and a matched velocity with $v_{pump}=v_{x\text{-}ray}$ (red spheres),.

The experiments were performed with the CPA Nd:glass laser system of the High Field Laser Application Laboratory at the Max-Born-Institute. This laser, operating at 1053nm wavelength, produces pulses with durations that can be varied between 0.7ps and 10ps in each shot. In the experiments, the CPA pulse was lengthened to ~ 6 ps with an energy of ~ 2.5J in the target chamber [51]. The pulse duration was monitored at each shot by a second-order autocorrelator, additionally the pulse shape was visualized by a OPCPA third order correlator. The X-ray laser output was analyzed by means of a flat-field grating spectrometer with a 1200-lines/mm Au-coated, Harada-type concave diffraction grating, coupled with a 16-bit back illuminated X-ray CCD camera. In order to produce fringes on the CCD detector, we used a pair of 5mm-wide slits placed 160 mm away from the target (see Fig.15). The double slit was oriented with the two slits parallel to the target surface and perpendicular to the direction of the entrance slit of the flat field spectrometer. We used a set of three different slit pairs with distances of 20, 40 and 60 μm between them. Fringe patterns of the x-ray laser were recorded by an x-ray CCD camera placed 480 mm away from the double-slit pair length target was 2.5 J in 6ps.

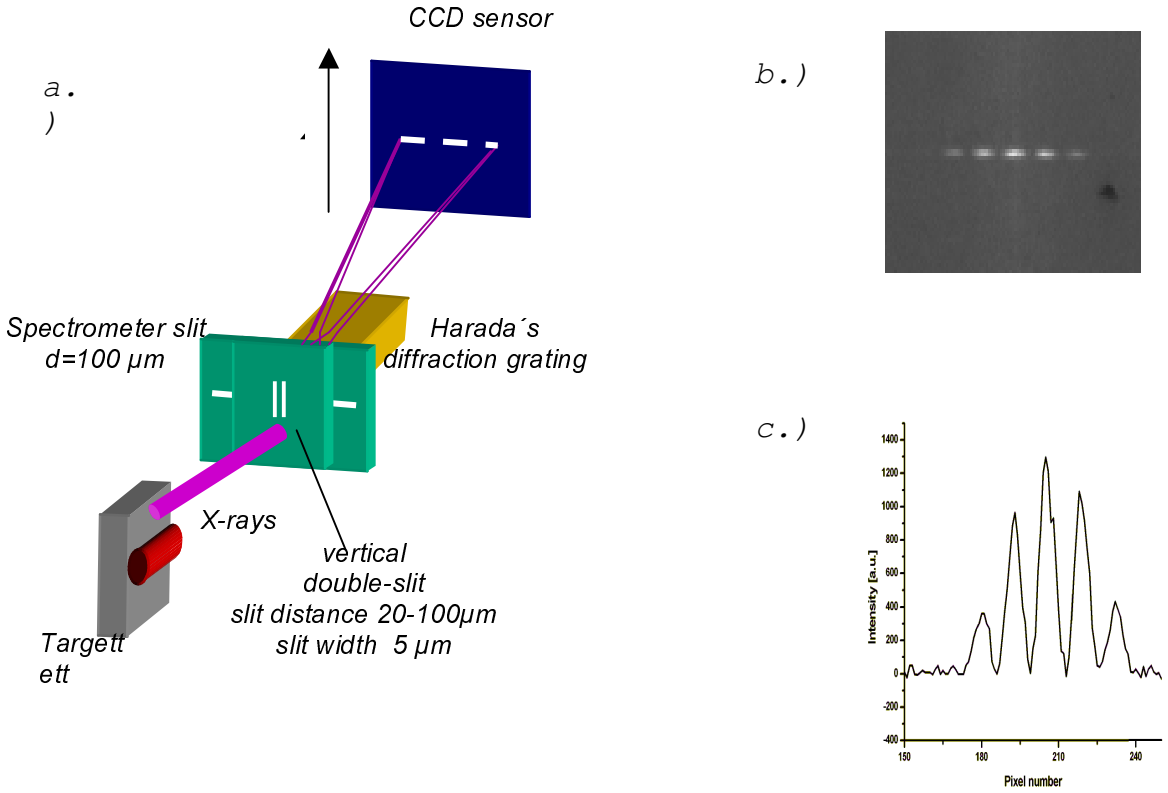

Figure 15: a.) Schematic representation of the experimental setup used in the (Youngs) double-slit interference coherence measurements. b.) Fringe pattern from a 20 mm separation slit pair for the 4d-4p, J = 0–1 line at 13.9nm in Ni-like Ag. The pump energy on the 6.7-mm *c*.) Line out of the fringe pattern showing full modulation of the fringes.

A typical example of the interferograms obtained from this experimental set-up with a target length of 6.7 mm is shown in Fig.15b. It has to be noted that with this target length the X-ray laser worked in the regime of saturated amplification with output energies in the µJ range. The distance between the slits is 20 µm. It illustrates the high visibility of the fringes, and the symmetric dependence of the visibility around the maximum along the slit direction. The fringe visibility, V, is defined as

$$V = \frac{I_{\max} - I_{\min}}{I_{\max} + I_{\min}} \tag{23}$$

pattern and the adjacent minimum intensity, respectively. The experimental determination of the visibility V allows to estimate the degree of spatial coherence of the X-ray laser radiation. For a quasi monochromatic light source the degree of spatial coherence is characterized by the cross correlation of fields across the output wavefront, which can be normalized to yield the complex coherence factor m [54]. In a double-slit interference experiment, where both slits are equally illuminated, the modulus of the complex coherence factor, |m|, is equal to the fringe visibility, V. The equality between |µ| and V is valid for every slit separation, Δx. Therefore

$$V(\Delta x) = |\mu(\Delta x)| \tag{24}$$

From the fringe visibility as a function of slit spacing, the diameter of the equivalent incoherent source of the x-ray laser can be calculated. The complex coherence factor as a function of the slit spacing is given by the Van Cittert-Zernike theorem [60] as

$$|\mu(\Delta x)| = 2 \bullet \frac{J_1(\pi d_S \Delta x / \lambda z)}{(\pi d_S \Delta x / \lambda z)} \qquad (25)$$

where Δx is the slit spacing, d_S is the diameter of the source, z the distance between the source and the double slit, and $J_1(x)$ is the Bessel function of the first kind, order 1. Figure 16 shows the experimental data of the visibility V as a function of the slit separation for the 4 mm and the 6.7mm target length. In Figure 16 results are given on the measurements of the fringe visibility for 20, 40 and 60μm slit-pair separations in a 4 mm and in a 6 mm length Ag target. The dashed line represents the fitting of the experimental data with a "least-square-fit" to the equation (25). An interesting and important point is that for both targets and 20 μm slit spacing, the fringe visibility reaches the unusually high value of 0.95. The values of the source diameter d_S obtained from the fitting are 23μm for both the 4 mm and the 6.7mm target length. This result shows for the first time that a collisional XRL can produce a high degree of spatial coherence at a few mm length of the amplifying medium. It is worth to note that our XRL output beam is generated with a high reproducibility of both saturation as well as of full spatial coherence. We interpret this behavior as a result of the specific irradiation conditions, which result in the production of a high amplifying plasma of good symmetry and homogeneity.

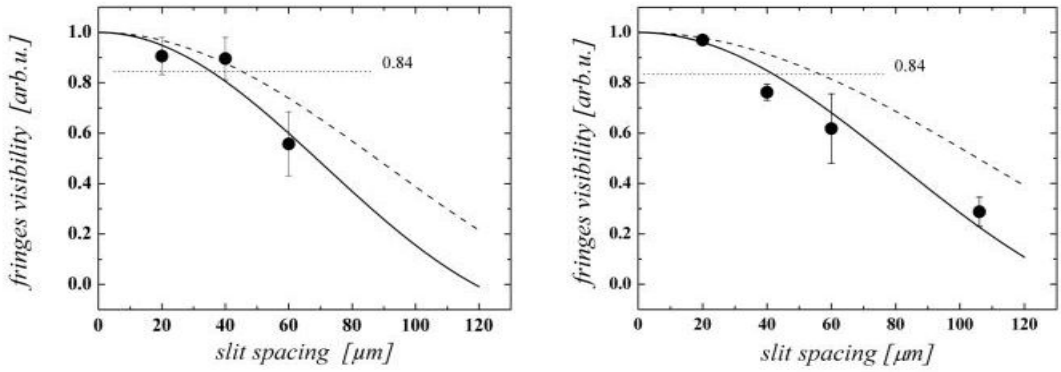

Fig.16: Measurement of the fringe visibility for 20, 40 and 60μm slit-pair separations in a 4 mm and in a 6 mm length Ag target. The dashed lines show the best fit, according to Eq. (25).

In summary, we have realized a compact and saturated nickel-like Ag X-ray laser at 13.9nm with a high degree of spatial coherence. This result, together with the low pump energy of less than 3J delivered in a single pulse, makes this XRL an attractive tool for applications in the physical and life sciences. The scalability of the required laser driver to still higher repetition rates will further increase the application potential of such XUV source with high peak brightness and moderate average power.

Additionally to the activities on collisionally excited X-ray lasers resulting in a saturated nickel-like Ag-XRL of high spatial coherence at 13.9nm, also first attempts have been made in order to look for amplification in recombination excited systems. For this purpose elongated moderate dense plasmas where produced using the capillary discharge technique (which failed in WP3 for the confinement of clusters). The capillary plasma is of a relatively cold temperature enableing thus the creation of a population inversion via an electron cascade produced by an ultra-intense fs-pulse. In the following we describe the first results of an optical field ionized recombination excited XRL pumped by a linearly polarized fs pump pulse.
This type of OFI-laser also requires (similarly to the conventional recombination scheme a high electron density ($n_e>10^{20}cm^{-3}$) and a very low temperature (Te<50eV). In the case of linearly polarized driving laser pulse the field ionization leaves the electrons a with relatively low energy. The most important process here in the creation of a population inversion is three-body electron-ion recombination that strongly depends on electron energy (temperature). The recombination rate is proportional to $T_e^{-9/2}$ [61,62]. In contrast to the conventional recombination laser (see recombination scheme cooling in the OFI XRL-plasma is in principle, not required, because field ionization produces low-energetic rapidly recombining electrons.
OFI-excitation allows for lasing down to the ground state of the lasant ions. However, nearly complete emptying of the ground state during ionization is required. Fractional population of 10-3 or greater remaining in the ground state can significantly reduce the predicted gain [63]. However, since ionization is strongly dependent on the intensity, only a modest increase in intensity above the ionization threshold is required to obtain nearly complete ionization. A disadvantage of lasing into the ground state are the slow exit channels out of the ground state resulting in a short duration of population inversion and a reduction in the saturation intensity. From another point of view this short life time of the population inversion has the advantage to result in very short XRL-output pulses.
One of the drawbacks of the present OFI-systems is their low energy efficiency (approximately $\eta\sim10^{-9}$). In the following our new results on the way to an optical field ionization recombination x-ray laser using linearly polarized laser light are introduced.

Enhancement of a 24.77 nm line emitted by plasma of boron-nitride capillary discharge irradiated by high-intensity ultrashort laser pulse

Investigations of plasma produced by a boron-nitride capillary discharge irradiated with a guided 20TW Ti-Sapphire laser pulse at peak intensity of $4x10^{18}W/cm^2$ are presented. The guided laser radiation in the plasma channel generated Li-like nitrogen ions and amplify a short-wavelength radiation at a wavelength of 24.77nm, indicating a possible lasing at the $3d_{5/2}–2p_{3/2}$ transition in Li-like nitrogen.
X-ray lasers hybrid schemes combining electric discharge and laser irradiation in one, were demonstrated in previous works [64,65]. The inherent advantage of this longitudinal arrangement as described above is an elongated medium efficiently pumped by a laser pulse during the guiding phase of the plasma channel created by the discharge [66,67-69]. However, the elongated medium increases both the absorption and ionization losses of the pump beam during the propagation. [70]. It was concluded, that an excess of the peak intensity, if compared to the threshold value of the expected ionization stage is necessary to ensure efficient and relatively uniform pumping along the plasma channel. It is well known that both recombination and collisional pumping schemes can be realized in such a plasma pipe provided that the optical field ionization (OFI) is the main mechanism in creation of highly ionized active medium [71]. The detailed analysis of the control over the plasma parameters

related to OFI-X-ray lasers is given in [72]. In the recent years a significant progress in development of the collisionally pumped OFI laser was demonstrated [65,73,74]. The recombination scheme applying the plasma pipes was successfully tested only for H-like lithium [64] but mostly with a limited output from a short medium due to the increased laser absorption losses. One of the most frequently discussed but never realized schemes was a recombination X-ray laser in Li-like nitrogen mainly due to the energy structure beneficial to reduction in the ATI residual energy [75,76]. In the present report we introduce strong enhancement of the 24.77 nm line in Li-like nitrogen (NV) obtained by irradiation of a boron-nitride (BN) capillary discharge plasma by a high intensity, ultra-short laser pulse at 810 nm. The possible explanation of the enhancement can be ascribed to lasing within the recombination pump scheme.

In the experiment the capillary discharge formed a pre-plasma and subsequently ionized by a short (FWHM~ 40 fs), linearly polarized laser pulse it by tunneling. The setup of the experiment is shown in Figure 17. The capillary was triggered by 20-30 mJ, 20 ns auxiliary Nd-YAG laser, after collinear alignment with the main laser pulse.[77, 78]. The jitter between the discharge and the main laser pulse was down to less than 5ns. The plasma was formed by discharging 0.05μF capacitor charged up to 5kV through 15 mm long BN capillary with diameter of 350μm. The discharge current monitored by a Rogowski coil had a half-cycle equal to 800ns with a rise time of 400ns. The current amplitude was between 500A and 650A. The temperature of the plasma formed by the discharge only, was estimated from the intensity ratio of two emission lines of ion BII at 345.1nm and 412.2nm measured by a Spectra Pro-275 Acton spectrograph coupled to the gated intensified photodiode array detector (IPDA). The system ensured the spectral resolution ~ 0.1nm and temporal resolution of 20nsec. It was found that the plasma temperature varies between 2.5 and 6eV during the first half-cycle of the current. An intense femtosecond pulse delivered into the capillary when the plasma temperature was between 4 and 6eV.

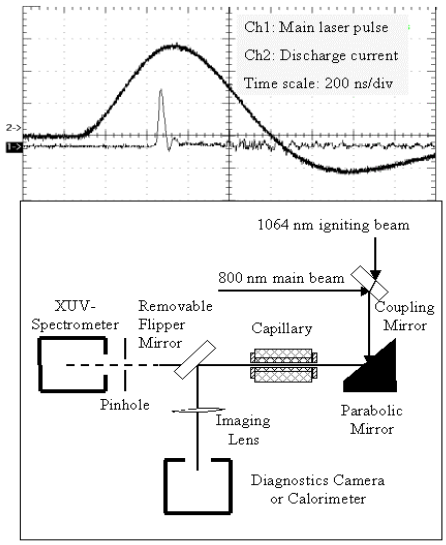

Figure 17: Experimental setup. Upper trace shows temporal history of the electrical parameters.

The short-wavelength spectrum of the plasma was recorded with a flat-field spectrometer consisting of Harada-type diffraction grating (1200 l/mm), multi-channel plate (MCP), phosphor screen and a cooled 16-bit back-illuminated CCD camera. The combination of the

MCP with the phosphor screen reduced slightly the system resolution but increased its sensitivity. Such a detector system required temporal gating of the acquisition process to reduce the long duration (if compared to sub-nanosecond scale of the processes of interest) emission of the discharge plasma. Here the gate duration was equal to 40ns. The spectrometer was calibrated with the OVI oxygen line at 17.3nm and a very closely situated (at 17.02nm) absorption edge of aluminum (Al) used as a filter with a leaf thickness of 300nm. The main pulse was focused with a f/1.5off-axis parabola (OAP) onto the capillary entrance. A flipper mirror was positioned closely to the capillary exit to enable a quick change from spectroscopic measurements to monitoring of guiding. The laser pulses applied in the described experiment were sufficiently short to avoid significant collisional heating even if the high electron density in the range of $2\times10^{19}cm^{-3}$ was expected on the capillary axis. The experimentally used peak intensity of the ionizing beam at the capillary entrance was equal to I_L~3-5×$10^{18}W/cm^2$. The 24.77 nm line intensity enhancement occurs at the time when only 20% laser energy was transmitted. The resulting spectra are shown in

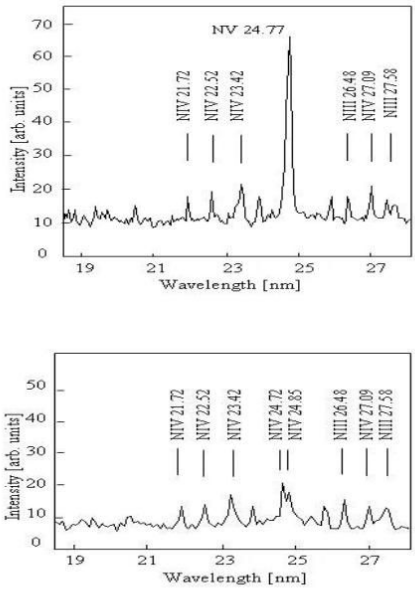

Figure 18: The spectrum of boron nitride plasma measured at 390nm delay relative to current beginning. a.) for capillary discharge irradiated by a femtosecond laser pulse b.) for pure capillary discharge.

Lower trace shows the temporally integrated (within the gate duration) emission spectrum of the non-irradiated plasma channel created by the discharge only. This spectra dominated by the nitrogen lines. There are no boron lines observed in the spectrum due to the low transition strengths of the lines present in the observed spectral range. The spectrum is dominated by the lines emitted by NIII and NIV ions indicating the average
Ionization ionization stage of Z^*=2.3 that corresponded to the measured plasma conditions. When this plasma irradiated with a very intense laser pulse its emission spectrum changed dramatically. A very strong line corresponding to the $3d_{5/2}$-$2p_{3/2}$ transition in Li-like nitrogen (NV) at 24.77nm was observed. This line was absent in the discharge spectrum. It is worth noting that the number of observed lines from NIV has been reduced, even if some of them became a bit stronger. This indicates an efficient ionization process. If this extremely strong increase in the line intensity was of thermal origin two other lines from NV ions emitting at 20.93 nm and 26.64nm corresponding to the transitions 3p–2s and 3s–2p, respectively, have

to be seen as well. These two lines emit in an equilibrium plasma with the intensity comparable (above 50%) with that of the 24.77nm line. However, they do not appear in the recorded spectrum of the irradiated plasma indicating possibility that lasing is responsible for observed effect. The very high laser intensity used in the experiment was capable to reach the required ionization level along the whole capillary length. This results from the fact that the maximum ionization stage available in medium was helium-like nitrogen (NVI) with the threshold intensity for ionization of $I_{th}(NVI)=1\times10^{19}W/cm^2$. This ionization stage is required to work within the recombination scheme with lithium-like ions (NV) ($I_{th}=1.5\times10^{16}W/cm^2$). It is clearly seen that the required ionization stage is stable in a wide range of intensities as the threshold intensity of NVI is significantly higher than the available laser peak intensity. A very high intensity being well above the relativistic limit ($I_L\approx10^{18}W/cm^2$) has been for the first time used in the experiment on recombination OFI-X-ray lasers.

In summary, we have demonstrated strong enhancement of the emission line at 24.77 nm corresponding to the $3d_{5/2} - 2p_{3/2}$ transition in Li-like nitrogen. An ultra high laser intensity was used to ionize quasi-uniformly the plasma channel during guiding. The high ionization level of the pre-plasma prevented the ionizing beam from too strong distortion caused by very intense ionization process. It has been shown that pump pulse shape can be deciding for reduction in the electron residual energy. Presently the output signal as function of the capillary length is investigated in order to determine the amplification factor according to the modified Linford formula.

Literature

[1] C. Wülker *et al*., *Phys Rev A,* (1994); T. Ditmire, J. W. G. Tisch, E. Springate, M. B. Mason, H. Hay, R. A. Smith, J. Marangos, M. H. R. Hutchinson, *Nature,* **386**, 54 (1997); A. McPherson, B. D. Thompson, A. B. Borisov, K. Boyer, C. K. Rhodes*, Nature, (London)* **370**, 631 (1994); K. Boyer, B. D. Thompson, A. McPherson, C. K. Rhodes, *J. Phys. B. At. Mol. Opt. Phys.*, **27**, 4373 (1994); T. Ditmire et al., *Phys. Rev. A*, **57**, 369 (1998)

[2] T. Mocek *et al., Phys. Rev. E*, **62**, 4461 (2000)

[3] P.V. Nickles, M. Kalachnikov, P. J.Warwick, K. A. Janulewicz, W. Sandner, U. Jahnke, D. Hilscher, M. Schnürer, R. Nolte, A. Rousse, *Quantum Electronics* (Russia), **29**, 444 (1999)

[4] M. Dammasch, priv. communication

[5] T. Wilhein, S. Rehbein, D. Hambach, M. Berglund, L. Rymell, H. M. Hertz, *Rev. Sci. Instrum.*, **70**, 1694 (1999)

[6] O. F. Hagena, W. Obert*, J. Chem. Phys.*, **56**, 1793 (1972)

[7] O. F. Hagena, Surf. Science, **106**, 101 (1981); O. F. Hagena, *Rev. Sci. Instrum.*, **63**, 2374 (1992)

[8] M. Visser *et al.*, *Emerging Lithographic Technologies III,* Proceed. of SPIE **3767**, 253 (1999)

[9] A.J. Bell, J.M. Mestdagh *et al.,J. Phys.D*, **26**, 994 (1993)

[10] L. Rayleigh, *The London Dublin Philosophic*, 375 (1899)

[11] M. Kerker, *The scattering of light and other electromagneticradiation*, Academic Press, New York, London (1969)

[12] H.P. Birkhofer *et al., Ber. Bunsenges., Phys. Chem*., **88**, 207 (1984)

[13] M. Lewerenz, B. Schilling, J. P. Toennies, *Chem. Phys. Lett.*, **206**, 381 (1993)

[14] R. Karnbach, M. Joppien, J. Stapelfeldt, J. Wormer, T. Moller, *Rev. Sci. Instrum*., **64**, 2838 (1993)

[15] T. Ditmire, R. A. Smith, J. W. G. Tisch, M. H. R. Hutchinson, *Phys. Rev. Lett.,* **78**, 3121 (1997)

[16] E. Miura, H. Honda, K. Katsura, E. Takahashi, K. Kondo, *Appl. Phys.*, **70**, 783 (2000)

[17] T. Ditmire, R. A. Smith, R. S. Majoribanks, G. Kulcsar, M. H. R. Hutchinson, *Appl. Phys. Lett.***, 71**, 166 (1997)

[18] K. Kondo, A. B. Borisov, C. Jordan, A. McPherson, W. A. Schroeder, K. Boyer, C. K. Rhodes*, J. Phys. B. At. Mol. Opt. Phys.*, **30**, 2707 (1997)

[19] J. Zweiback, T. Ditmire, and M. D. Perry, *Phys. Rev. A***, 59**, R3166 (1999)

[20] G. O'Sullivan, *J. Phys. B***, 15**, L765 (1982)

[21] M. McGeoch, *Appl. Opt.*, **37**, 1651 (1998)

[22] H. Fiedorowicz, A. Bartnik, M. Szczurek, H. Daido, N. Sakaya, V. Kmetik, Y. Kato, M. Suzuki, M. Matsumura, J. Tajima, T. Nakayama, Th. Wilhein, *Opt. Com.,* **163**, 103 (1999)

[23] M. A. Klosner, W. T. Silvfast, *J. Opt. Soc. Am. B*, **17**, 1279 (2000)

[24] H. Honda, E. Miura, K. Katsura, E. Takahashi, K. Kondo, *Phys. Rev. A*, **61,** (2000); B. A. M. Hansson, L. Rymell, M. Berglund, H. M. Hertz, *Microel. Engin.*, **53**, 667 (2000)

[25] T. Ditmire, T. Donnelly, A. M. Rubenchik, R. W. Falcone, M. D. Perry, *Phys. Rev. A,* **53**, 3379 (1996)

[26] ULR: http://www-cxro.lbl.gov

[27] J. Underwood, in *Extrem Ultraviolet Lithography*, G. Kubiak, D. Kania, eds., **vol.4** of *Trends in Optics and Photonics Series* (Optical Society of America, Washington, D. C., 1996), pp.162-166; G. D. Kubiak, L. J. Bernardez, and Kevin Krenz, Proceedings *SPIE*, **3331**, 81 (2000)

[28] M. Lezius, S. Dobosz, D. Normand, M. Schmidt, *Phys. Rev. Lett.*, **80**, 261 (1998)

[29]N. H. Burnett, P. B. Corkum, *J.Opt. Soc. Am. B*, **6**, 1195 (1989)

[30] W. Lotz, *Z. Phys*., **216**, 241 (1968)

[31] P. B. Corkum, N. H. Burnett, F. Brunel, *Phys. Rev. Lett.,* **62**, 1259 (1989)
[32] G. Pretzler and E. E. Fill, *Phys. Rev. **E**,* **56**, 2112 (1997)
[33] E. E. Fill, *J.Opt. Soc. Am. B, **11***, 2241 (1994)
[34] G. J. Pert, *J. Phys. B: At. Mol. Opt. Phys.,* **32**, 27 (1999)
[35] V. Kumarappan, M. Krishnamurthy, D. Mathur, and L. C. Tribedi, *Phys. Rev. **A**,* **63**, 3203 (2001)
[36] I. Will *et al*., *IEEE J Quant. Electron.*, **34**, 2020 (1998)
[37] R.Doron, E. Behar, P. Mandelbaum, J. L. Schwob, H. Fiedorowicz, A. Bartnik, R. Jarocki, M. Szczurek and T. Wilhein, *Phys. Rev. A*, **59**, 188 (1999)
[38] T. Ditmire, P. K. Palet, R. A. Smith, J. S. Wark, S. J. Rose, D. Milathianaki, R. S. Majoribanks, and M.H. R. Hutchinson, *J. Phys. B: At. Mol. Opt. Phys*., **31**, 2825 (1998)
[39] U. Vogt, H. Stiel, I. Will, P.V. Nickles, W. Sandner, M. Wieland, and T. Wilhein, *Appl. Phys. Lett.***, 79,** 2336 (2001)
[40] S. Kranzusch and K. Mann, *Opt. Commun*., **200**, 223 (2001)
[41] M.Mori, T.Shiraishi, E.Takahashi, H.Suzuki, L.B.Sharma, E.Miura, and K.Kondo, *J. Appl. Phys.*, **90**, 3595 (2001)
[42] M.Schnurer, S. Ter-Avetisyan, H. Stiel, U. Vogt, W. Radlof, M. Kalashnikov, W. Sandner, and P.V. Nickles, *Eur. Phys. J. D*, **14**, 331 (2001)
[43] G. Kooijiman, R de Bruijn, K. Koshelev, F. Bijkerk, W. Shaikh, A. J. Bodey, G. Hirst, „*Prepulse enhanced EUV yield from a xenon gas-jet laser produced plasma"*, Central Laser Facility Annual Report 2001/2002, Rutherford, UK, published online: http://www.clf.rl.ac.uk/Reports/2001-2002/contents.html
[44] S. Eliezer, *The interaction of high-power lasers with plasmas* (IOP, London) p.323 (2002)
[45] P. V. Nickles, M. Schnürer, H. Stiel, U. Vogt, S. Ter-Avetisyan and W. Sandner., *Proceed. SPIE* ,. **4504**, 106 (2001)
[46] E.Parra, I. Alexeev, J.Fan, K.Y.Kim, S.J.McNaught and H.M.Milchberg, *Phys. Rev. Lett.*, **62**, R5931 (2000)
[47] S.Ter-Avetisyan, M.Schnurer, H. Stiel, U. Vogt, W. Radlof, M. Kalashnikov, W. Sandner, and P.V. Nickles, *Phys. Rev. E*, **64**, 036404 (2001)
[48] D. A. Tichenor, G. D. Kubiak, W. C. Replogle, L. E. Klebanoff, J. B. Wronosky, L. C. Hale, H. N. Chapman, J. S. Taylor, J. A. Folta, C. Montcalm, R. M. Hudyma, K. A. Goldberg, P. Naulleau, SPIE, **3997,** 48 (2000)
[49] B. A. M. Hansson, M. Berglund, O. Hembers, H. M. Hertz, *Proceed. SPIE***, 3997,** 729 (2000)
[50] R. Lebert *et al*., *Comparison of different source concepts for EUVL*, *Proceed. SPIE*, **4343**, (2001)
[51] K.A. Janulewicz,. Lucianetti, G.Priebe, W. Sandner, and P.V. Nickles, *Phys. Rev.A*, (2004)
[52] P.V. Nickles, K.A. Janulewicz, F. Bortolotto *et al*., *Proc. SPIE*, Denver (2000); K.A. Janulewicz, J.J. Rocca, F. Bortolotto *et al*., *C.R.Acad. Scien*.,**1**, Ser IV, 1083 (2000)
[53] J. L. A. Chilla and J.J. Rocca, *J. Opt. Soc. Am. B,* **13**, pp. 2841-2851 (1996)
[54] S. Le Pape *et al*., *Phys Rev. Lett.,* **88**, 183901 (2002)
[55] H. Daido *et al*, '*X-ray Laser 2002'*, Proceedings of the 8th International Conference on X-ray Lasers in Aspen, Colorado, AIP Conference Proceeedings, vol. **641**, pp.473-480 (2002).
[56] R. E. Burge *et al*., *J. Opt. Soc. Am. B***, 14**,. 2742-2751 (1997)
[57] M.C. Marconi et al., *Phys. Rev. Lett.*, **79**, 2799 (1997)
[58] Y. Liu et al., *Phys. Rev. A*, **63**, 033802 (2001)
[59] P. Lu *et al*., *Phys. Rev. A*, **58**, 628 (1998)
[60] J.W. Goodman, *Statistical Optics*, John Wiley & Sons, New York, 1985

[61] Y. Zeldovich, Y. Raizer, *"Physics of Shock Waves and High-Temperature Hydrodynamic Phenomena"*, Academic , New York, 1966, pp. 406-413
[62] G.J. Pert, *J. Phys. B*, **23**, 619(1990)
[63] D.C. Eder, P. Amendt, S.C. Wilks, *Phys. Rev. A*, **45**, 6761 (1992)
[64] A. Goltsov, A. Morozov, S. Suckewer, R. Elton, U. Feldman, K. Krushelnick, T. Jones, C. Moore, J. Seely, P. Sprangle, A. Ting, and A. Zigler, *IEEE J. Sel. Top. Quantum Electron*., **5**, 1453 (1999)
[65] A. Butler, A.J. Gonsalves, C.M. McKenna, D.J. Spence,S.M. Hooker,S. Sebban, T. Mocek, I. Bettaibi, B. Cros, *Phys. Rev. Lett.,* **91**, 205001 (2003)
[66] P. Sprangle and E. Essarey, *Phys.Fluids B*, **4**, 2241 (1992)
[67] D.C. Eder, *et.al*, *Phys. Plasmas*, **1**, 1744 (1994)
[68] M.J. Grout, K.A. Janulewicz, S.B. Healy, and G.J. Pert, *Opt. Commun*., **141**, 213 (1997)
[69] Y. Ehrlich, C. Cohen, D. Kaganovich, A. Zigler, R.F. Hubbard, P. Sprangle, E. Esarey, *J. Opt. Soc. Am. B*,**15**, 2416 (1998)
[70] D.J. Spence, S.M. Hooker, *J. Opt. Soc. Am. B*, **17**, 1565 (2000)
[71] I. Geltner, Y. Ping, S. Suckewer, J. Opt. Soc. Am. B, 20, 616 (2003)
[72] K.A. Janulewicz, J.J. Rocca, F. Bortolotto, A. Lucianetti, N. Bobrova, P.V. Sasorov, W. Sandner, P.V. Nickles, *J. Opt. Soc. Am. B*, **20**, 215 (2003).
[73] N.H. Burnett, P.B. Corkum, *J. Opt. Soc. Am. B*, **6**, 1195 (1989).
[74] G.J. Pert, *J. Phys. B*, **34**, 881 (2001).
[75] B.E. Lemoff, G.Y. Yin, C.L. Gordon III, C.P.J. Barty, and S.E. Harris, *Phys. Rev. Lett*., **74**, 1574 (1995).
[76] S. Sebban *et. al*, *Phys. Rev. Lett*., **86**, 3004 (2001).
[77] 15. B. Greenberg, M. Levin, A. Pukhov, and A. Zigler, *Appl. Phys. Lett*., **83**, 2961 (2003).
[78] J.A. Koch *et al*, *Phys. Rev. Lett*., **68**, 3291 (1992)

II.2. Voraussichtlicher Nutzens, insbesondere die Verwertbarkeit des Ergebnisses im Sinne des fortgeschriebenen Verwertungsplanes

The results of the work on EUV-emission of Xe-clusters have shown, that Xe^{7+}-Xe^{11+} gives the main contribution to the 13.4 nm emission. At long ns-pulses and intensities between 10^{11}-10^{12}W/cm^2 an optimum conversion efficiency can be reached. This result is very important for the realization of an industrial 150W 13.4 nm source for lithography applications, since these requirements seems to be soon coverable by new commercially available state f the art pump lasers with high repetition rate. The efficiency scaling can also be used for other Xe-targets like Xe-jets. The maximum efficiency value of 0.8% for circularly polarized highly intense fs laser pulses shows another possibil*i*ty to further increase the efficiency, even if at the moment corresponding fs CPA lasers are still far from industrial use.
The X-ray laser results using a shaped ps-pulse show the possibility of down-sizing the XRL drivers, which could result in the next future in a stable working X-ray laser with high averaged power, due to pump lasers with repetition rate. The spatial coherence of such a system is already now usable for various applications.
At the moment there are no industrial applications identifiable.

II.3 Während der Durchführung bekannt gewordener Fortschritt

During the period of the project work activities have been started in industrial laboratories with Xe-jets (based on experiences with Xe gas and clusters) to realize an EUV source according to the lithography roadmap. Results are only partly published. Additionally also other target systems for the 11nm band are under consideration. Recently Nishimura (private communication) has shown a conversion efficiency up to 2% using Ti-foam targets. However it is not clear whether the 11nm emission band could gain an importance for industrial application due to the necessity of multilayers containing Be.

II.4 Veröffentlichungen

- M. Schnürer, S. Ter-Avetisyan, H. Stiel, U. Vogt, W. Radloff, M. Kalachnikov, W. Sandner, and P. V. Nickles “Influence of laser pulse width on absolute EUV-yield from Xe-clusters”. Eur. Phys. J. D 14, 331-335 (2001).

- S. Ter-Avetisyan, M. Schnürer, H. Stiel, U. Voigt, W. Radloff, W. Karpov, W. Sandner, and P. V. Nickles “Absolute EUV-yield from fs laser excited Xe-clusters”. Phys. Rev. E 64, 036404 (2001).

- P. V. Nickles, M. Schnürer, H. Stiel, U. Vogt, S. Ter-Avetisyan and W. Sandner “Absolute EUV-yield of laser-irradiated Xe-clusters in dependence on the pulse width”. SPIE Proc. 4504, 106-113 (2001)
- M. Schnürer, H. Stiel, U. Vogt, S. Avetisyan, I. Will, M. P. Kalachnikov, W. Radloff, P. Nickles and W. Sandner “Laser-plasma sources for extreme ultraviolet (EUV) lithography”. Laser Opto 33 (3), 50-6 (2001).

- H. Stiel, U. Vogt, S. Ter-Avetisyan, M. Schnürer, I. Will, and P. V. Nickles “EUV-emission of Xenon-clusters excited by a high repetition rate burst mode laser” SPIE Proc. 4781, 26-34(Bellingham 2002).

- P.V. Nickles, S. Ter-Avetisyan, H. Stiel, W. Sandner, and M. Schnürer "Absolute X-ray yield studies from Xe-clusters with ultrashort Ti:sapphire laser pulses at $2x10^{18}$ W/cm^2" in: AIP Conferences Proceedings Vol 611(1) (Melville, New York, 2002 New York 2002) pp. 288-293.

- S. Ter-Avetisyan, U. Vogt, H. Stiel, M. Schnürer, I. Will, and P.V. Nickles "Efficient EUV emission from Xenon-cluster jet targets at high repetition rate laser illumination" Journal of Applied Physics 94, 5489-5496 (2003).

- K. A. Janulewicz, G. Priebe, A. Lucianetti, R. Krömer, W. Sandner, R. E. King, G. J. Pert, P. V. Nickles, "Output characteristics of a transient Ni-like Ag soft X-ray laser pumped by a single picosecond laser probe",*SPIE Proc.* **, 5197**, 90-98 (2003)

- P.V. Nickles, K. A. Janulewicz, G. Priebe, A. Lucianetti, R. Krömer, A. K. Gerlitzke, W. Sandner, "Status of MBI activities - Will transient collisional X-ray laser with high repetition rate came soon?", *SPIE Proc*., **5197**, 29-37 (2003)

-K. A. Janulewicz, A. Lucianetti, G. Priebe, W. Sandner, P. V. Nickles, "Saturated Ni-like Ag X-ray laser at 13.9 nm pumped by a single picosecond laser pulse", *Phys. Rev. A*, **68**, 051802-5 (2003)

- K. A. Janulewicz, F. Bortolotto, A. Lucianetti, W. Sandner, P. V. Nickles, J. J. Rocca, N. Bobrova, P. V. Sasorov, "Fast capillary discharge plasma as a preformed medium for longitudinally pumped collisional x-ray lasers", *J. Opt. Soc. Am. B*, **20**, 215-220 (2003)

- K. A. Janulewicz, A. Lucianetti, W. Sandner, P. V. Nickles,"X-ray lasers at MBI", Laser Technology VII: Progress in Lasers, *SPIE Proceedings*, **5230**, 189-194 (2003)

- K. A. Janulewicz, A. Lucianetti, G. Priebe, P. V. Nickles,"Review of state-of-the-art and about characteristics table-top sof X-ray lasers" *X-ray Spectrometry*, **33**, 262-266 (2004)

- K. A. Janulewicz, P. V. Nickles, R. E. King, G. J. Pert, "Influence of pump pulse structure on a transient collisionally pumped Ni-like Ag X-ray laser", *Phys. Rev. A*, **70**, 013804/1-7 (2004)

- A. Lucianetti, K. A. Janulewicz, R. Kroemer, G. Priebe, J. Tümmler, W. Sandner, P. V. Nickles, V. I. Redkorechev, "Transverse spatial coherence of a transient nickellike silver soft-x-ray laser pumped by a single picosecond laser pulse", *Opt. Lett.,* **29**, 881-883 (2004)

- K.A. Janulewicz, G. Priebe, J. Tümmler, P.V. Nickles," Single-pulse low-energy-driven transient inversion X-ray lasers", IEEE J. Sel. Top. Quant. Electron., (in press)

- K.A. Janulewicz, Matthias Schnürer, Johannes Tümmler, Gerd Priebe, Enrico Risse, Peter V. Nickles, Boris Greenberg, Misha Levin, Anatoly Pukhov, Pinchas Mandelbaum, Arie Zigler, "Enhancement of a 24.77 nm line emitted by plasma of boron-nitride capillary discharge irradiated by high-intensity ultrashort laser pulse", Opt. Lett., (in press)

III. Kurzer Erfolgskontrollbericht

III.1 Beitrag des Ergebnisses zu förderpolitischen Massnahmen

The project activities have shown both the potentials (and limitations) of laser driven short pulse EUV- and X-ray sources on the base of large Xe-clusters and collisional x-ray lasers. The results allows one to scale requirements for pumping laser systems necessary for scientific and industrial applications of these incoherent respectively coherent sources

III.2 Wissenschaftlich-technische Ergebnisse

Large Xe–clusters (10^5-10^6 atoms per cluster) have been exposed with ultrashort (50fs) and high intensity (2–4)×10^{18}W/cm^2 pulses from a Ti:Sa-laser. Scaling and absolute yield measurements of EUV–emission in a wavelength range between 7nm and 15nm in combination with cluster target characterization demonstrate the role of cluster size, average density and target configuration for yield optimization. Maximum emission in the 11nm to 13nm emission band has been found with backing pressures between 5 and 15 bar. The registered anisotropy of on-axis and off-axis emission suggests an important influence of the source size, ion distribution and radiation absorption within the ambient cluster gas. A simple model of a possible source geometry can explain main features of the observed signals. With the laser parameters used here Xe^{9+}-Xe^{11+}–ions are produced via optical field ionization and are probably not essentially covered by further collisions. Therefore the use of circularly polarized laser light results in enhancement of the radiation signals in comparison to linearly polarized light. An absolute emission efficiency up to 0.5% in 2π sr at about 13.4nm wavelength and 2.2% bandwidth was realized. With longer 30 ps–10 ns laser pulses at moderate intensities (<10^{15}W/cm^2) could also be demonstrated an efficient conversion of the laser energy in to EUV-emission. For the Xe-plasma a high conversion efficiency of 0.2% (2π sr, 2.2%BW) in to 13.4nm radiation was measured at laser pulse duration of 30ps and an intensity of 10^{15}W/cm^2. It is especially important that in case of 10ns laser pulses at 10^{14} W/cm^2 a still higher conversion efficiency of 0.26% (2π sr, 2.2 % BW) could be reached. In general, the radiation efficiency rises with increasing intensity. It was shown that the Xe-cluster jet target having a high flow velocity is well suited for efficient EUV-emission with high repetition of up to 125kHz. Both the high conversion efficiency and the high repetition rate make this type of Xe-target attractive for high average EUV-power sources. Based on available laser technology, further technical and application requirements can be chosen for a suitable Xe–target system for bright EUV–radiation. As a coherent source we have realized a compact and saturated nickel-like Ag X-ray laser at 13.9nm with a high degree of spatial coherence. This result, together with the low pump energy of less than 3J delivered in a single pulse, makes this XRL an attractive tool for applications in the physical and life sciences. The scalability of the required laser driver to still higher repetition rates will further increase the application potential of such XUV source with high peak brightness and moderate average power.
Additionally it was demonstrated a strong enhancement of the emission line at 24.77 nm corresponding to the $3d_{5/2}$ –$2p_{3/2}$ transition in Li-like nitrogen created in a capillary discharge plasma using a well-developed technology of our israeli project partners. An ultra high laser intensity was used to ionize quasi-uniformly the plasma channel during guiding. The high ionization level of the pre-plasma prevented the ionizing beam from too strong distortion caused by very intense ionization process. It has been shown that pump pulse shape can be deciding for reduction in the electron residual energy. This result could open a way for both

the recombination as well as collisional excited x-ray lasers characterized by low pump energy and high pointing stability. The latter could have importance for many applications.

The most part of the experimental environment is on site. Cluster nozzles, discharge capillaries, diagnostics a.o. are still available. The work on the x-ray lasers is being continued.

III.3 Fortschreibung des Verwertungsplans

The published results on incoherent X-ray and especially EUV-emission of Xe-clusters could certainly help to find more industrial related solutions for a high average power 13 nm lithography source. However these activities have been more and more moved to the specific laboratories of the big players like Phillips, Jenoptik a.o.
The result on the collisionally pumped Ag-X-ray laser has a potential for future applications supposing a further reduction of the pump energy could be demonstrated, which would allow the use of pump lasers with high repetition rate. Such lasers are under development and especially the new thin-disk laser technology could open the way for such drivers. Therefore we are trying to collaborate with the group of Dr. Giesen from Institute of Strahlwerkzeuge, University Stuttgart, who has pioneered the thin-disk laser development, in order to realize a corresponding kHz driver laser. A kHz-X-ray laser could be a interesting small-sized complementary coherent bright source to the Tesla free electron laser facility which will be commissioned in 2007 in Hamburg.

III.4 Arbeiten, die zu keiner Lösung geführt haben

It must be noted that the high-risk topic-confinement of clusters in a discharge capillary to create a efficiently excited elongated plasma column as active media for a future x-ray laser-failed. The reason was the difficulty to create stable clusters in the capillary geometry and keep them stable enough for an irradiation with a short laser pulse.

III.5 Präsentationsmöglichkeiten für Nutzer

The most part of the experimental environment is on site. Cluster nozzles, discharge capillaries, diagnostics a.o. are still available. The work on the x-ray lasers is being continued.

III. 6 Einhaltung der Ausgaben und Zeitplanung

The work on project was finished under full consideration of the temporal as well as finance planning.